HIGH MASS STAR FORMATION IN NORMAL LATE-TYPE GALAXIES: OBSERVATIONAL CONSTRAINTS TO THE IMF

A. BOSELLI[1], S. BOISSIER[1], L. CORTESE[2], V. BUAT[1], T.M. HUGHES[2] G. GAVAZZI[3]
Draft version November 4, 2021

ABSTRACT

We use Hα and far-ultraviolet (FUV, 1539 Å) GALEX data for a large sample of nearby objects to study the high mass ($m \geq 2$ M⊙) star formation activity of normal late-type galaxies. The data are corrected for dust attenuation using the most accurate techniques at present available, namely the Balmer decrement for Hα data and the total far-infrared to FUV flux ratio for GALEX data. The sample shows a highly dispersed distribution in the Hα to FUV flux ratio (Log $f(H\alpha)/f(FUV) = 1.10 \pm 0.34$ Å) indicating that two of the most commonly used star formation tracers give star formation rates with uncertainties up to a factor of 2-3. The high dispersion is partly due to the presence of AGN, where the UV and the Hα emission can be contaminated by nuclear activity, highly inclined galaxies, for which the applied extinction corrections are probably inaccurate, or starburst galaxies, where the stationarity in the star formation history required for transforming Hα and UV luminosities into star formation rates is not satisfied. Excluding these objects, normal late-type galaxies have Log $f(H\alpha)/f(FUV) = 0.94 \pm 0.16$ Å, which corresponds to an uncertainty of ∼ 50% on the SFR. The Hα to FUV flux ratio of the observed galaxies increases with their total stellar mass. If limited to normal star forming galaxies, however, this relationship reduces to a weak trend that might be totally removed using different extinction correction recipes. In these objects the Hα to FUV flux ratio seems also barely related with the FUV-H colour, the H band effective surface brightness, the total star formation activity and the gas fraction. The data are consistent with a Kroupa (2001) and Salpeter initial mass function in the high mass stellar range ($m > 2$ M⊙) and imply, for a Salpeter IMF, that the variations of the slope γ cannot exceed 0.25, from $\gamma = 2.35$ for massive galaxies to $\gamma = 2.60$ in low luminosity systems. We show however that these observed trends, if real, can be due to the different micro history of star formation in massive galaxies with respect to dwarf systems.

Subject headings: Galaxies: general; Galaxies: spiral; Galaxies: evolution; Galaxies: fundamental parameters; Stars: formation; (ISM): HII regions

1. INTRODUCTION

The formation and evolution of galaxies can be observationally constrained through the study of their present and past star formation activity. While the star formation history of galaxies can be well determined by fitting their stellar ultraviolet (UV) to near-infrared spectral energy distribution with population synthesis models, the direct observation of the youngest high mass stars is generally used to infer their ongoing activity. The present day star formation rate (SFR) is generally determined using the luminosity of the youngest stars and the relation $SFR = K(\lambda) L(\lambda)$, where $K(\lambda)$ can be inferred from population synthesis models under several assumptions (see Kennicutt 1998 for a review). Hydrogen Balmer emission lines and UV fluxes, both related with the emission of the youngest stellar populations, are thus often used as direct tracers of the present day star formation activity of galaxies. This widely used technique can be blindly applied only if the initial mass function (IMF) is universal, thus independent of morphological type, luminosity and redshift and if the star formation activity of the target galaxies has been constant for a time ≥ than

the lifetime of the emitting stars, i.e. ∼ 10^7 years for Balmer emission lines and a few 10^8 years for the UV ($\lambda < 2000$ Å).

Direct measurements of the IMF in the Milky Way or in other very nearby galaxies (Massey et al. 1995; Scalo 1998; Selman & Melnick 2008) are consistent with a universal IMF (e.g. Scalo 1986; Kroupa 2001; Renzini 2005). A few recent indirect observational results on the mass to light ratio of low surface brightness galaxies (Lee et al. 2004), on the SED properties of SDSS (Hoversten & Galzebrook 2008) and starburst (Rieke et al. 1993) galaxies, on the Hα to UV flux ratio of nearby objects (Meurer et al. 2009) as well as on the star formation activity vs. stellar mass assembly in the far universe (Davé 2008; Wilkins et al. 2008), combined with theoretical (Krumholz & McKee 2008) and statistical considerations (Pflamm-Altenburg et al. 2007) led several authors to question this statement. These works suggest that the IMF, in particular when considered as a unique function representative of the whole galaxy, might not be universal but rather changing with the galaxy stellar mass, the star formation activity or the gas column density. The IMF is a key parameter in the process of star formation: proving its non universality would thus have enormous implications on the study of the star formation process at all scales, from the physics of the interstellar medium to the formation and evolution of galaxies since the earliest phases of the universe. Indeed the IMF is a

[1] Laboratoire d'Astrophysique de Marseille, UMR 6110 CNRS, 38 rue F. Joliot-Curie, F-13388 Marseille France
[2] School of Physics and Astronomy, Cardiff University, 5, The Parade, Cardiff CF24 3YB, UK
[3] Universita degli Studi di Milano-Bicocca, Piazza delle Scienze 3, 20126 Milano, Italy

key ingredient in all models of galaxy evolution.

It should also be tested whether the condition of stationarity in star formation, required for transforming Hα and UV fluxes into star formation rates, is satisfied in all kinds of galaxies. There are indeed some indications that this is not the case: it has been shown that a bursty history of star formation is expected in dwarf galaxies (Fioc & Rocca-Volmerange 1999), consistent with the determination of the star formation history obtained using the stellar colour-magnitude diagram of dwarf galaxies in the local group (e.g. Mateo 1998). A recent starburst activity has been also proposed to explain the the Hα to UV flux ratio of UV luminous galaxies (Sullivan et al. 2000). It is thus time to investigate whether these two assumptions on the constancy of the star formation history of late-type galaxies and on the universality of the IMF are consistent with the latest observational data in our hands. The comparison of the star formation activity determined using independent indicators of a well defined sample of galaxies with a complete dataset of Hα, UV and IR imaging and optical ($R \sim 1000$) integrated spectroscopy allows us to quantify the uncertainty associated to different tracers. Furthermore since the ratio of the number of ionizing and non-ionizing photons emitted by a galaxy depends on the slope and on the upper mass cutoff of the IMF, on its present and past star formation activity and on its metallicity, the Hα to UV flux ratio (properly corrected for dust attenuation) can be used to constrain the shape of the IMF.

Determining the UV ionizing and non-ionizing emitted radiation through observations is however extremely difficult since at these wavelengths the emission of galaxies is severely attenuated by the dust of the interstellar medium. Both UV continuum and Balmer line data need thus to be corrected for dust attenuation. Quantifying the dust attenuation of the UV radiation is still one of the major challenges in modern astronomy. Models and observations have recently shown that dust extinction can be well determined considering that the UV radiation absorbed by dust is re-emitted in the far-IR (Buat & Xu 1996; Witt & Gordon 2000; Buat et al. 2002; Boselli et al. 2003; Cortese et al. 2008). At the same time the attenuation of the Balmer lines can be determined using the Balmer decrement (e.g. Lequeux et al. 1981). This is generally done by comparing the observed to the nominal Hα to Hβ flux ratio, this last being fairly constant with a value of 2.86 (case B, Osterbrock 1989), provided that spectroscopic data have a sufficient resolution for deblending the [NII] from Hα and for accurately measuring the underlying Balmer absorption. The ionizing radiation could also be absorbed by dust or escape the galaxy before ionizing the gas. All these phenomena should be taken into account in the determination of the emitted radiation using observational data.

The study of the shape of the IMF using Hα and UV data was first proposed by Buat et al. (1987) and later adopted by Meurer et al. (1999), Boselli et al. (2001) and Charlot et al. (2002). Although limited by the statistics of their sample and by the lack of corollary data for accurate extinction corrections, all these works agreed with a constant IMF. The advent of the GALEX mission (Martin et al. 2005), which provided us with homogeneous UV data for thousands of objects, and the availability of high quality integrated spectroscopy for hundreds of galaxies in the nearby universe (Kennicutt 1992; Jansen et al. 2000; Gavazzi et al. 2004; Moustakas & Kennicutt 2006) with IR data, are providing us with a unique opportunity to revisit this subject with a new dataset. The work of Salim et al. (2007), based on GALEX data and SDSS spectra, or that of Meurer et al. (2009) suggested that the Hα to UV flux ratio could indeed vary with stellar mass.

The aim of the present work is to study the high mass star formation activity of normal, late-type galaxies. The paper is structured as follows: in sect. 2 we give a brief description of the sample, in sect. 3 of the dataset. The analysis and the discussion are given in sect. 4 and 5 respectively. A detailed description of the observational data (A), of the derived parameters (B) used in the analysis with their uncertainties (C) and on possible selection biases (D) are presented in the Appendix.

2. THE SAMPLE

The analysis presented in this work is based on three samples of late-type nearby galaxies with available Hα and UV data: the Herschel Reference Survey (Boselli et al. 2009), which is a K band selected ($K_{Stot} \leq 12$ mag), volume limited ($15 < Dist < 25$ Mpc) sample of galaxies, the Virgo cluster sample extracted from the Virgo Cluster Catalogue (VCC) of Binggeli et al. (1985), an optically selected sample complete to $m_B \leq 18$ mag ($M_B \leq -13$), and the UV Atlas of galaxies of Gil de Paz et al. (2007).

To exclude those objects whose interaction with the cluster environment might have perturbed and modified their star formation history, we removed all galaxies with an HI-deficiency > 0.4 (Boselli & Gavazzi 2006). The interaction with the cluster environment might indeed change the Hα over UV flux ratio (Iglesias-Paramo et al. 2004) as in the case of the anemic galaxy NGC 4569 (Boselli et al. 2006). For the same reason we also excluded strongly interacting or merging galaxies belonging to the GALEX UV atlas.

The resulting sample, not complete in any sense, includes thus 198 galaxies with Hα and FUV data (see Table 1) and spans a large range in morphological type (from Sa to Sm, Im and BCD) and luminosity (-22 < M_B < -13). Dwarf systems (-15 < M_B < -13) are present only in the Virgo cluster sample.

Distances are determined assuming galaxies in Hubble flow with H_0 = 75 km s^{-1} Mpc^{-1} except for Virgo cluster objects where distances are taken according to Gavazzi et al. (1999).

3. THE DATA

The study of the high mass star formation activity of nearby, late-type galaxies is based on the analysis of their Hα and UV emission. All sample galaxies thus have narrow band Hα and broad band GALEX imaging data. Multifrequency imaging (optical, near-IR and far-IR) and spectroscopy (optical, HI and CO) data are also necessary to derive the different entities used in the following analysis, such as stellar masses, metallicities, effective surface brightnesses, colours, gas column densities and deficiencies (see the Appendix B).

Hα imaging data are corrected for [NII] contamination and dust extinction using long slit, integrated spec-

troscopy with a resolution $R \sim 1000$, optimal for deblending [NII] from Hα and for resolving the underlying Hβ absorption. If spectroscopic data are not available, then Hα imaging data are corrected for [NII] contamination and dust attenuation using standard, luminosity dependent statistical relationships (see the Appendix B). UV GALEX data are corrected for dust extinction using the prescriptions of Cortese et al. (2008) based on TIR/FUV flux ratio whenever IRAS far-IR data are available, or using standard recipes based on the UV spectral slope or H band effective surface brightness in other cases (Cortese et al. 2006).

The analyzed sample can thus be divided into three different subsamples according to the quality of the available data (see Table 2). The *high quality sample* (H.Q.) includes 111 galaxies for which the Balmer decrement and the TIR/FUV flux ratio guarantee the best possible dust extinction correction. The *medium quality sample* (M.Q.) is formed by 148 galaxies[4] includes also objects where dust extinction has been corrected using the Balmer decrement for the Hα imaging data and indirect, empirical relationships for the FUV fluxes whenever TIR data are not available. The *low quality sample* (L.Q.) includes in addition galaxies for which both Hα and UV data have been corrected using statistical and indirect relations. This last sample includes 198 objects. Details on the adopted dust extinction corrections and on the different derived parameters used in the following analysis (metallicities, stellar masses and star formation rates) are given in the Appendix B. The Appendix (C) also gives an estimate of the errors on the different variables, with a discussion on possible biases in the data (D).

4. ANALYSIS

The Hα luminosity gives a measure of the global photoionization rate of the interstellar medium due to high mass ($m > 10$ M$\odot$), young ($\leq 10^7$ years) O-B stars (Kennicutt 1998). Assuming that the SFR of galaxies is constant on a time scale comparable to the life time of the stellar population responsible for the ionizing emission (a few 10^7 years), the SFR is proportional to the Hα luminosity. The UV emission of a galaxy at 1500-2300 Å is dominated by the emission of less recent ($\sim 10^8$ years) and massive ($2 < m < 5$ M$\odot$) A stars (Lequeux 1988). The UV emission becomes stationary if the SFR is constant over $\sim 10^8$ years in FUV (e.g., Boissier et al., 2008). In that case the relatively high mass star formation activity of a galaxy is proportional to the FUV luminosity. Whenever the star formation activity is constant over $\sim 10^8$ years, the Hα to FUV flux ratio is proportional to the ratio of the number of ionizing to non-ionizing massive stars and is thus directly related to the shape of the IMF in the high mass star range ($m > 2$ M$\odot$). To simplify the analysis, we assume that the fraction of ionizing photons that escape the galaxies before ionizing the gas (escape fraction) is zero. We also assume that the fraction of ionizing photons absorbed by dust before ionizing the gas is zero (f=1).

The top panel of Fig. 1 shows the distribution of the Hα over FUV flux ratio for the whole sample (dashed line). The first interesting result is that the dispersion

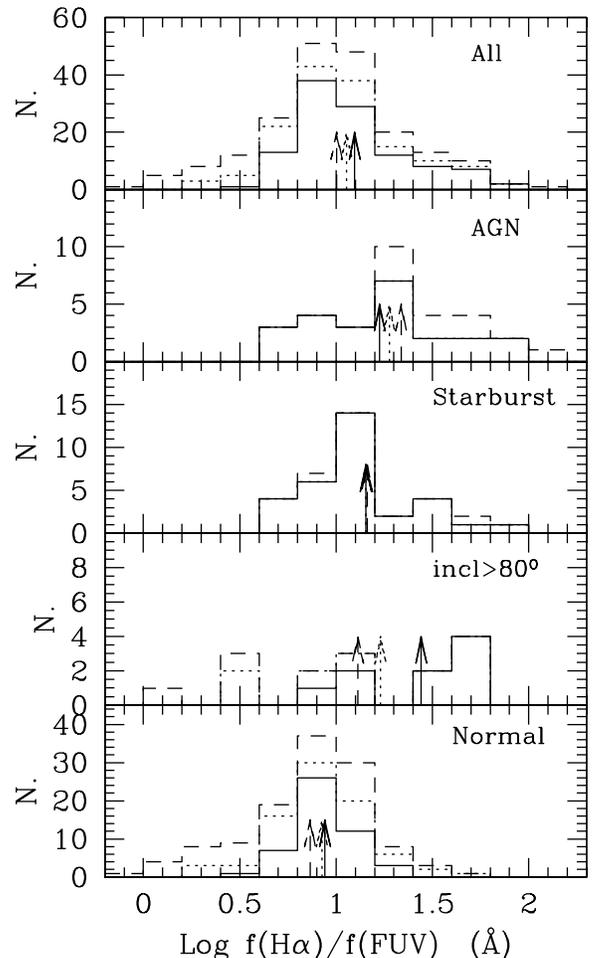[4] H.Q $\subset$ M.Q. $\subset$ L.Q.

FIG. 1.— The Hα to FUV flux ratio distribution (in logarithmic scale) for galaxies with high quality (solid line), medium quality (dotted line) and all (dashed line) dust extinction corrections. From top to bottom, all sample galaxies, AGNs, starbursts, galaxies with an inclination > 80 ^{o} and normal galaxies used in the analysis of the IMF. The vertical arrows indicate the mean values of the distributions (see Table 3).

in the distribution of the selected galaxies is quite large even when we limit this estimate to the high quality sample (0.34 dex, solid line, see Table 3), for which uncertainties due to dust extinction corrections are less severe. Since this large dispersion might be due to the presence of AGNs (where part of the global Hα and UV emission might not be related to star formation and where the [NII] contamination to the narrow band imaging data is probably more uncertain than in normal galaxies), starbursts (where star formation is known to vary on short time scales) or highly inclined galaxies (where the extinction correction are highly uncertain), we separate the sample in four different subsamples: AGNs (Seyfert 1 and 2, LINER), starbursts (defined as those galaxies with a 60 over 100 μm IRAS flux ratio $F(60)/F(100) > 0.5$, Rowan-Robinson & Crawford 1989), edge-on galaxies (with an inclination $> 80^o$, but

including also the other highly inclined objects listed in Table 4) and the remaining star forming galaxies ($F(60)/F(100)\leq0.5$, inclination $\leq 80^o$, non AGN), that hereafter we call "normal" to differentiate them from those belonging to the previous categories. The dispersion of the Hα over FUV flux ratio of normal, star forming galaxies (0.16 dex) is, as expected, significantly reduced with respect to the original sample. Despite their small number, highly inclined galaxies have the highest Hα to FUV flux ratio (Log $f(H\alpha)/f(FUV) = 1.44 \pm 0.32$ Å). Most of them have prominent dust lanes, as indicated in Table 4. This result is in agreement with Panuzzo et al. (2003) and Tuffs et al. (2004) who used dust models for different geometries. They claimed that standard recipes for dust extinction correction calibrated on face-on or low inclination galaxies underestimate $A(FUV)$ in edge-on systems. AGNs, and in a minor way, starbursts also have Hα to FUV flux ratios larger than normal galaxies (see Table 3). A Kolmogorov-Smirnov test has shown that the probability that the distribution of Log $f(H\alpha)/f(FUV)$ for AGN, starbursts and inclined galaxies is similar to that of "normal" galaxies is 1%, 34% and 2% respectively.

4.1. The Hα to FUV vs. M_{star} relation

Several observational evidences indicate that the galaxy mass is the most important parameter driving galaxy evolution (Cowie et al. 1996; Gavazzi et al. 1996; Boselli et al. 2001; Gavazzi et al. 2002b). Figure 2 shows a relationship between Log $f(H\alpha)/f(FUV)$ and the galaxy stellar mass (compared to the constant ratio determined for a Salpeter[5] IMF using the calibration of Kennicutt 1998, black solid line), with massive galaxies having on average a higher ratio than dwarfs (Table 5) with however considerable scatter. This relation is still present when only high quality data are used (big filled symbols), but it is significantly reduced (the dynamic range in Log $f(H\alpha)/f(FUV)$ drops from ~ 1.4 to ~ 0.3; see below) if highly inclined (magenta triangles), AGN (cyan pentagons) and starburst galaxies (orange diamonds) are not considered.

Using SDSS spectroscopy and UV GALEX data of a large sample of star forming galaxies Salim et al. (2007) found a similar trend between the Hα over FUV ratio and the total stellar mass of galaxies. They imputed their result as due to an inaccurate dust extinction correction based on standard Charlot & Fall (2000) models calibrated on the UV slope. The trend observed in our sample (~ 1.4 dex) is more important than that of Salim et al. (2007) which is ~ 0.5 dex within a mass range $10^9 \leq M_{star} \leq 10^{11}$ M$\odot$ probably because of the larger dynamic range in stellar mass of our sample ($10^7 \leq M_{star} \leq 10^{11}$ M$\odot$) and the presence of AGN, excluded in Salim et al. (2007). Finally, a trend between the Hα to UV flux ratio and the R band luminosity or the rotational velocity of the galaxies has been found by Meurer et al. (2009), with an amplitude (~ 1 in dex) comparable to ours. A similar dependence of the Hα to FUV flux ratio
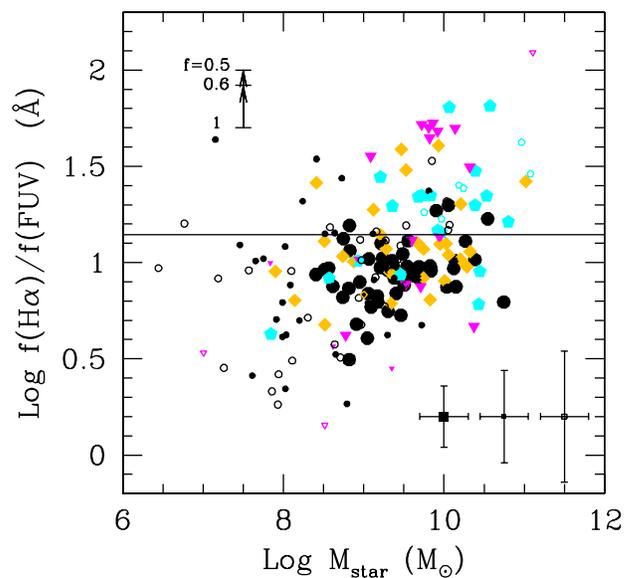

FIG. 2.— The relationship between the Hα to FUV flux ratio and the total stellar mass (both in logarithmic scales) for all galaxies in the sample, in units of erg cm^{-2} s^{-1} (Hα) and erg cm^{-2} s^{-1} Å^{-1} (FUV). Large filled symbols are for the high quality sample, small filled symbols for the medium quality sample and small empty symbols for the low quality sample. Magenta triangles are for highly inclined ($incl > 80^o$) galaxies, including those objects listed in Table 4, orange diamonds for starburst ($F60/F100 > 0.5$) galaxies, cyan pentagons for AGNs, while black symbols for "normal" galaxies. The solid line gives the expected ratio for the standard Kennicutt (1998) values. The vertical black arrows give the Y-axis shifts expected for different corrections considering the fraction of ionizing photons absorbed by dust ($f =1$ is for no correction). The error bars give the typical uncertainties for galaxies in the high, medium and low quality samples.

with the B band absolute magnitude or the star formation rate has been shown by Lee et al. (2009) on a nearby sample dominated by dwarf galaxies. While Salim et al. (2007) imputed the observed trend to an inaccurate dust extinction correction, Meurer et al. (2009) interpreted it as a clear evidence of a varying IMF with galaxy mass. Lee et al. (2009) concluded that, although the data are consistent with a changing IMF, other causes can be at the origin of the observed trend.

5. DISCUSSION

---

[5] Although never directly measured down to the hydrogen burning limit, a Salpeter IMF is used as reference throughtout the paper since generally used in extragalactic studies.

The observed variation of the Hα over FUV flux ratio as a function of the galaxy stellar mass might have different origins: it might be due to an inaccurate dust attenuation correction, to a variation of the escape fraction and dust absorption of ionizing photons, to metallicity effects, to the lack of stationarity for the star formation activity over the last few million years, or to a variation of the IMF. With the aim of reducing as much as possible the degrees of freedom in the adopted dataset, we exclude from the following analysis all those objects where the determination of the corrected Hα and FUV fluxes can be complicated by the presence of active galactic nuclei (AGN), extremely inclined galaxies ($incl > 80^o$), where the extinction correction is known to be problematic, and starburst galaxies, where the star formation activity is known to vary on short time scales. As previously shown (Fig. 1) these galaxies have an Hα to FUV flux ratio significantly different than that of normal, star forming objects. We thus focus our attention to the "normal" galaxy sample, for which a trend between the Hα to FUV flux ratio and the stellar mass seems still present (black symbols in Fig. 2).

5.1. Dust extinction

Extinction corrections for both the FUV and Hα data are still the highest source of uncertainty in the determination of the emitted Hα over FUV flux ratio even in normal galaxies. We should thus be sure that the observed trends shown in the previous figures do not result from any systematic effect in the applied corrections. To see whether extinction corrections can be at the origin of the observed trend in Fig. 2, we plot in Fig. 3 the relationship between the Log of the Hα to FUV flux ratio and the Log of the stellar mass using data corrected following different dust attenuation recipes. To reduce the uncertainties, we limit this comparison to the high quality sample. The plotted relationships are for: a) observed entities, b) Hα and FUV data corrected for dust attenuation as described in the present work (Balmer decrement for Hα and the TIR/FUV calibration of Cortese et al. 2008 for the FUV), c) Hα data corrected using the Balmer decrement and FUV data corrected following the prescription for starburst galaxies of Calzetti (2001): $A(FUV) = 1.78 A(H\alpha)$, d) Hα data corrected using the luminosity dependent statistical relation given in the Appendix B and FUV data corrected as described in this work, e) Hα data corrected using the Balmer decrement and FUV data corrected using the TIR/FUV vs. FUV-NUV relation given by Muñoz-Mateos et al. (2009) obtained for normal, late-type galaxies, $L_{TIR}/L_{FUV} = 10^{0.30+1.15(FUV-NUV)} - 1.64$, combined with the $A(FUV)$ vs. L_{TIR}/L_{FUV} relationship given by Buat et al. (2005), and finally f) Hα data corrected using the luminosity dependent statistical relation given in the Appendix B and FUV data using the FUV-NUV colour index as in e). The corrections used in f) are analogues to those adopted by Meurer et al. (2009), where $A(H\alpha)$ is determined from an $A(H\alpha)$ vs. R band luminosity relation and $A(FUV)$ using a L_{TIR}/L_{FUV} vs. FUV-NUV relation. The corrections in d) and e) are analogues to the Meurer et al. (2009) method for $A(H\alpha)$ and $A(FUV)$ respectively.

Figure 3 and Table 6 show that a trend in the Hα to FUV flux ratio vs. M_{star} relationship is present, although with a large scatter and a small dynamic range (~ 0.6 dex) when uncorrected data are used (a). The steepness of the relationship is reduced when data are corrected using our recipes (b), and are totally removed when FUV data are corrected using the Calzetti's law (c). Opposite to this, a very tight relationship is observed when a luminosity dependent correction for the Hα data is adopted (d), while a dispersed trend similar to that present in the observed data is seen when the FUV data are corrected using a recipe based on the FUV-NUV colour (e). The combination of a luminosity dependent correction for Hα and a FUV-NUV colour dependent correction for FUV data introduces a strong and tight correlation between the Hα to FUV flux ratio and the galaxy stellar mass (f) (see Table 6).

This comparison indicates that adopting the statistical, luminosity dependent extinction correction given in the Appendix B and shown in Fig. 14 for the Hα data is unsuited since it introduces systematic effects in the data. This is quite obvious given that the H band luminosity (from which $A(H\alpha)$ is determined) is strongly correlated to the galaxy stellar mass. The Balmer decrement is thus the most critical parameter for determining the emitted Hα to FUV flux ratio. The low quality sample is thus totally unreliable for any statistical study and will thus not be used in the following analysis. Corrections of the FUV data based on the FUV-NUV colour[6] (e) do not introduce any systematic effect since here they conserve the same trend present in the observed data. For this reason the medium quality sample could still be used, although with caution, in the analysis. Once the Balmer decrement is available, the adoption of different recipes for correcting the FUV data can maintain (e), reduce (b) or remove (c) the observed trend between Log $f(H\alpha)/f(FUV)$ and Log M_{star}. This means that any observed variation of the Hα to FUV flux ratio with other galaxy parameters might result from systematic effects introduced by the adopted correction and should thus be considered with extreme caution. As a first consideration we can say that the relationships between the Hα to FUV flux ratio and the R band luminosity or the rotational velocity (which is tightly related with the total mass of galaxies through the virial theorem) shown by Meurer et al. (2009) can result from their adopted corrections, in particular the Hα one which is determined using an $A(H\alpha)$ vs. L_R relation. In a more indirect way, the trend between Hα to FUV flux ratio and the R band or Hα surface brightness shown in Meurer et al. (2009) might also be affected by the adopted corrections since the surface brightness of the old and young stellar populations are also tightly related to the total mass of galaxies (Gavazzi et al. 1996). To conclude, for constraining the high mass star formation activity of late-type galaxies high quality, medium resolution integrated spectroscopy (for determining the Balmer decrement and the Hα to [NII] ratio) is mandatory. To a minor extent, IR data necessary for correcting UV fluxes are also necessary.

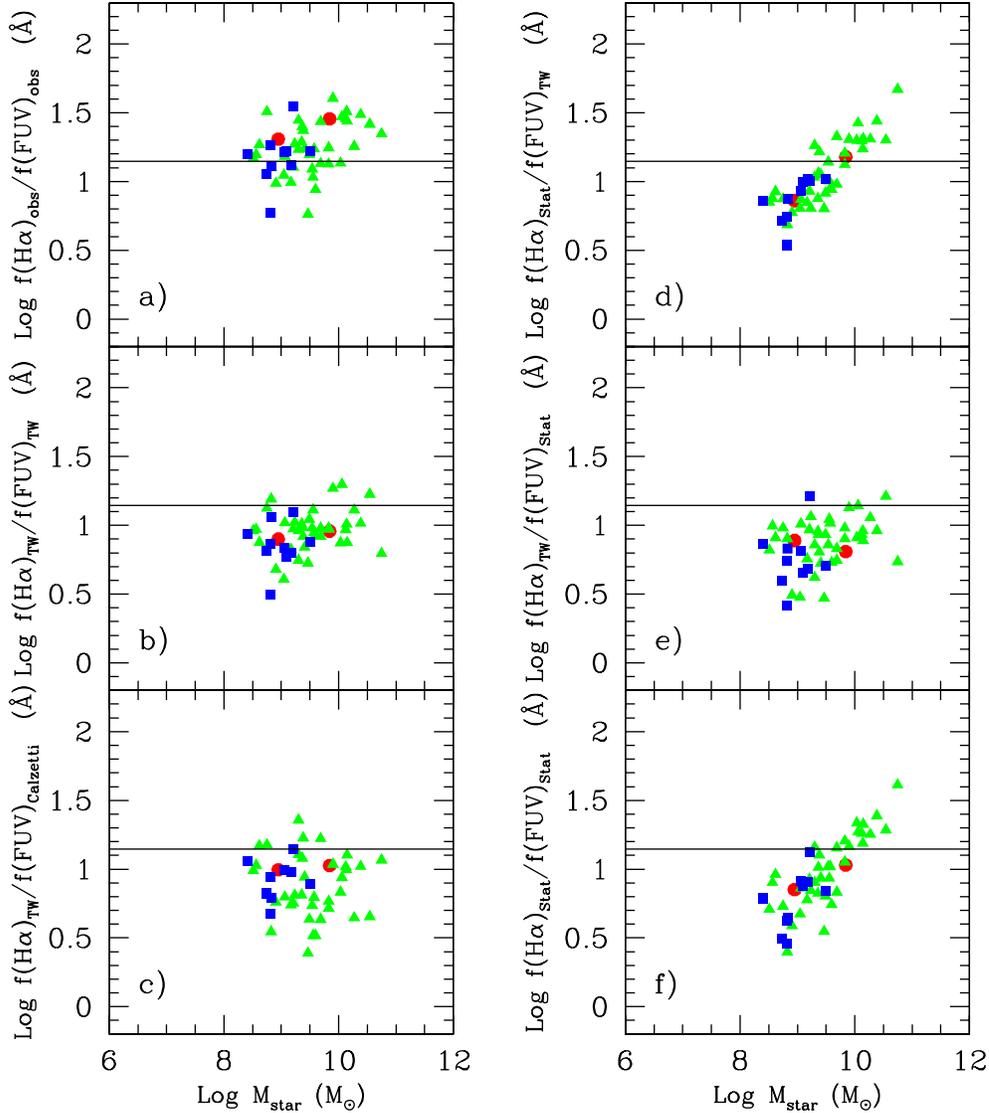[6] These are the corrections generally used in the medium quality sample

FIG. 3.— The relationship between the Hα to FUV flux ratio and the stellar mass (both in logarithmic scales) for "normal" galaxies belonging to the high quality sample, where the suffix "obs" stands for observed entities, "TW" for the standard corrections applied in this work, "Calzetti" for corrections based on the Calzetti's law and "Stat" for statistical corrections similar to those used by Meurer et al. (2009) (see text). The solid, horizontal line gives the expected ratio for the Kennicutt (1998) calibrations. Red circles are for Sa-Sb, green triangles for Sbc-Sd and blue squares for Sm-Im-BCD galaxies. The best fit to the data are given in Table 6.

The correction recipes adopted in this work are likely the more reliable to date since directly based on the TIR to FUV ratio of normal spirals and not on empirical relations (e) or calibrated on starburst galaxies (c) (see Buat et al. 2002). We remind however that even in our recipes global FUV-optical/near-infrared colours are needed to convert the TIR/FUV ratio into A(FUV). Thus we cannot completely exclude that a weak "spurious" trend in colour (and perhaps in stellar mass) is introduced by the dust corrections technique here adopted.

Once corrected adopting our recipes (Cortese et al. 2008), the Hα to FUV flux ratio still shows a very weak trend with stellar mass, with massive objects having slightly higher values of Log $f(H\alpha)/f(FUV)$ than dwarfs (0.14 dex), as shown in Table 5. The Spearman probability that the two variables are correlated is however weak (94%) (8). The dynamic range covered by Log$f(H\alpha)/f(FUV)$ is comparable to the statistical un-

certainty on this variable (see the Appendix C). It is thus impossible to state whether the observed trend is real or due to systematic effects related to the adopted extinction correction. A complete set of multiwavelength data for dwarf galaxies is necessary for extending the dynamic range in stellar mass and thus proving the real existence of this relationship. Lee et al. (2009) have recently done a similar analysis on a sample of nearby galaxies in the local universe using a set of multifrequency data similar to ours (Hα narrow band imaging and FUV GALEX fluxes, corrected for extinction using integrated spectroscopy and far-IR data). Their analysis has shown that the Hα to FUV flux ratio decreases in low luminosity systems (their sample includes galaxies down to $M_B \sim$ -12, while our is mostly limited to $M_B \sim$ -15). A tentative extension of our analysis to the low luminosity regime can be done by adding the medium quality sample, for which Balmer decrement measure-
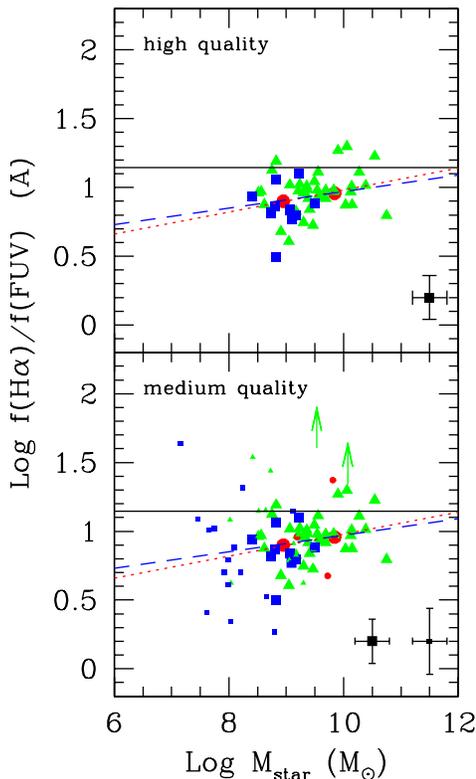
FIG. 4.— The relationship between the Hα to FUV flux ratio and the stellar mass (both in logarithmic scales) for "normal" galaxies belonging to the high quality sample (upper panel; big symbols) and to the medium quality sample (lower panel; small symbols). The solid, horizontal line gives the expected ratio for the Kennicutt (1998) calibrations, the red, dotted line the best fit to the high quality sample and the blue, dashed line to the medium quality sample (see Table 8). Red circles are for Sa-Sb, green triangles for Sbc-Sd and blue squares for Sm-Im-BCD galaxies.

ments are available. As shown in Table 8 and in Figure 4, the relationship between the Hα to FUV flux ratio and M_{star} (and $(FUV - H)_{AB}$ and $\mu_e(H)_{AB}$, see next Sect.) extends also to the medium quality sample at the same significance level. At the same time statistical considerations (see Sect. 5.5.1) predict that the integrated IMF of a given galaxy is truncated at high masses whenever its global star formation is low, as is the case in dwarf systems. We thus consider the Hα to FUV flux ratio vs. M_{star} relation as real, and we try to understand its origin.

5.1.1. Dust absorption of the ionizing radiation

In the case that dust is mixed with gas, only a fraction of the Lyman continuum photons (f) produced in the star forming regions contributes to the ionization of the atomic hydrogen, the remaining (1-f) being absorbed by dust (e.g. Inoue et al. 2000). The determination of f from an observational point of view is quite problematic since it requires the knowledge of the exact number of ionizing and non-ionizing UV photons produced by the different stellar populations inhabiting a galaxy. Here we measure f by comparing the mean ratio of the observed Hα to FUV flux of massive galaxies to the expected values for different population synthesis models [7]. Hirashita et al. (2003), using a relatively small sample of star forming galaxies with both Hα and UV (2000 Å) measurements, concluded that f is ∼ 0.57 for a Salpeter IMF in the mass range 0.1< m <100 M⊙, a value that they found almost independent on metallicity (Hirashita et al. 2001). The $f(H\alpha)/f(FUV)$ flux ratio of normal, massive galaxies (Log$f(H\alpha)/f(FUV)$ = 1.03 ± 0.16 Å) corresponds to the expected value for a Salpeter IMF using the Kennicutt (1998) calibration (Log$f(H\alpha)/f(FUV)$ = 1.15 Å) if f = 0.77. Different values of f are obtained for other IMF, as listed in Table 7, or for a given IMF in different ranges of stellar mass. The values of f determined here are larger than that of Hirashita et al. (2003), and range from ∼ 1 to 0.77 for a Salpeter IMF. It is quite unlikely that the observed trend between the Hα to FUV flux ratio and the stellar mass in normal, star forming galaxies (black symbols in Fig. 2) is due to a decreasing f with stellar mass since, given the strong metallicity-luminosity relation, we expect that the fraction of ionizing photons absorbed by dust is more important in massive galaxies than in metal poor dwarfs.

5.2. Lyman continuum escape fraction

A fraction of the Lyman continuum photons can escape galaxies without ionizing the surrounding hydrogen. This effect has to be considered in the determination of the emitted ionizing radiation using Hα observed fluxes. Direct measurements of the escape fraction based on the observations of the Lyman continuum photons are available only for starburst galaxies: they all indicate that the escape fraction is ≤ 6 % (e.g. Leitherer et al. 1995 (< 3%), Heckman et al. 2001 (≤ 6%), Deharveng et al. 2001 (≤ 6%); Hayes et al. 2007 (3%)). By measuring the ionizing radiation of the Magellanic stream, Bland-Hawthorn & Maloney (1999) have estimated that the escape fraction of the Milky Way is ≈ 6%. This value is consistent with the poorly constrained upper limit given by Zurita et al. (2000) (≤ 50%) determined by measuring the contribution of the diffuse gas to the ionizing radiation of spiral discs. Given these small values (≤ 6%), we confidently think that a mass dependent variation of the Lyman continuum escape fraction may not entirely cause the observed trend between the Hα to FUV flux ratio and the galaxy stellar mass (Fig. 2).

5.3. Metallicity

Stellar population synthesis models indicate that the Hα to FUV flux ratio might change with metallicity. Variations of ∼ 30 % in Hα and ∼ 20 % in FUV (Bicker

---

[7] Only massive galaxies are used since these are the only objects for which the required stationarity condition for star formation is guaranteed (see Sect. 5.4.2).
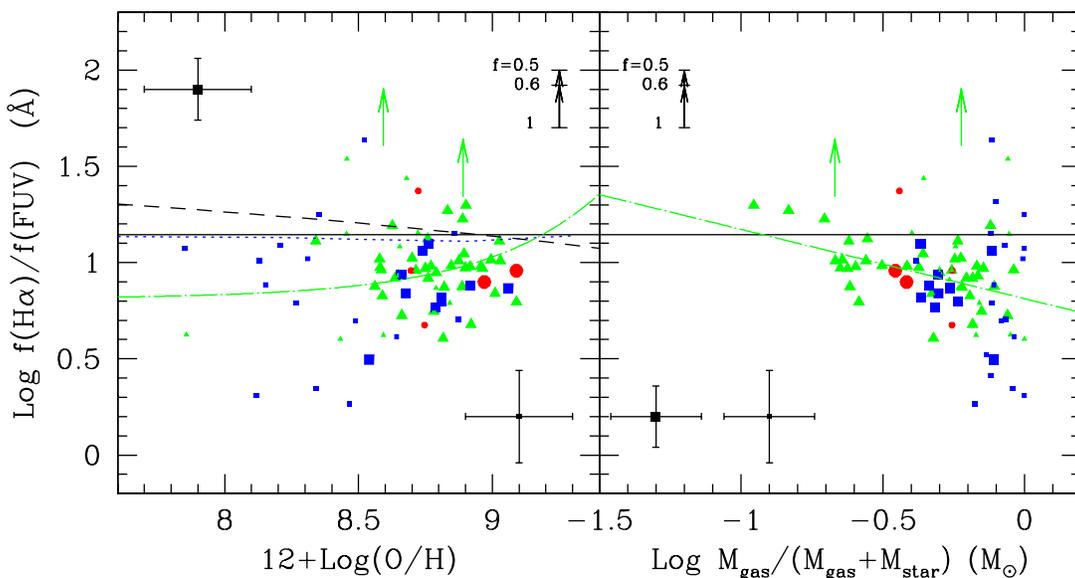
FIG. 5.— The relationship between the Hα to FUV flux ratio and the 12 + Log(O/H) metallicity index (left) and the gas mass fraction (right) for normal, late-type galaxies in the high (large, filled symbols) and medium (small filled symbols) quality samples. Red circles are for Sa-Sb, green triangles for Sbc-Sd and blue squares for Sm-Im-BCD galaxies. The error bars give the typical uncertainties for galaxies in the high and medium quality samples. The solid, horizontal line gives the expected ratio for the Kennicutt (1998) calibration, the blue dotted line for the metallicity dependent models of Bicker & Fritze-Alvensleben (2005) and the black dashed line for the metallicity dependent models of Vasquez et al. (2007) in the case that rotation of massive stars is taken in consideration. The green, long dashed-dotted line shows the expected dependence of Log $f(H\alpha)/f(FUV)$ on 12+Log(O/H) (left panel) considering the observed relationship between Log $f(H\alpha)/f(FUV)$ and the gas fraction (right panel; see Table 8).

& Fritze-Alvensleben 2005) are expected for metallicities between 1 and 1/50 solar. The effects of metallicity on the $f(H\alpha)/f(FUV)$ ratio, however, are minor since they neutralize themselves in the ratio. In the case that the rotation of massive stars is taken in consideration (Vázquez et al. 2007), however, the Hα flux can change up to ~ 30 % while the FUV flux by only a few % in FUV.

Figure 5 shows the relationship between the $f(H\alpha)/f(FUV)$ ratio and the galaxy metallicity (12+Log(O/H)). No relation is observed between the two variables (see Table 8). The variation of the Hα to FUV flux ratio predicted by the models in the range of metallicity of the sample galaxies is significantly smaller than the dispersion in the data. In a closed box model, the gas mass fraction, defined as $(M_{gas}/(M_{gas}+M_{star}))$,

is tightly related to metallicity (Garnett 2002). The total gas content of our sample galaxies can be determined by adding the HI measurement to the molecular hydrogen (when not available, we consider $M(H_2) = 15\% \ M(HI)$, Boselli et al. 2002b) and considering 30% of helium. Figure 5 shows a relationship between $f(H\alpha)/f(FUV)$ and the total gas fraction $(M_{gas}/(M_{gas}+M_{star}))$, with lower values observed in those objects with higher gas fractions. We use the relation in Table 8 (green dotted-dashed line in right panel) and combine it with gas fraction-metallicity relation for a close box model $(Z = -p\ln(M_{gas}/(M_{gas}+M_{star}))$, where p is the oxygen yield; Garnett 2002), to predict the dependence of Log$f(H\alpha)/f(FUV)$ on 12+Log(O/H) (green, dashed-dotted line in left panel). We find that the relatively loose trend with the gas fraction is consistent with
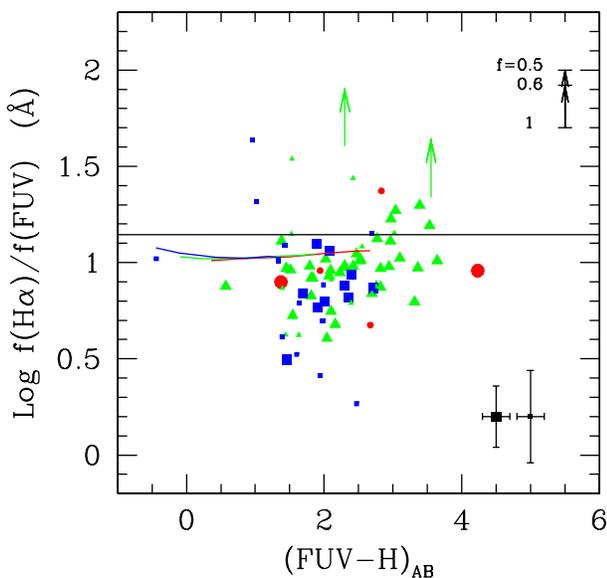
FIG. 6.— The relationship between the Hα to FUV flux ratio and the extinction corrected FUV-H colour index (in AB system) for normal, late-type galaxies. Symbols are coded as in Fig. 5. The coloured solid lines are for our multizone, chemospectrophotometric models of galaxy evolution for galaxies with different spin parameters (red: $\lambda = 0.02$, compact galaxies, green: $\lambda = 0.05$, standard galaxies, blue: $\lambda = 0.09$, low surface brightness galaxies). .

the observed scatter in the $\mathrm{Log}f(H\alpha)/f(FUV)$ vs. metallicity plot.

Although normal galaxies follow a well known luminosity-metallicity relation (Zaritsky et al. 1994; Tremonti et al. 2004) we can exclude that the trend shown in Fig. 3 is due to metallicity since population synthesis models predict lower values of the Hα to FUV flux ratio for metal rich, massive galaxies, contrary to what is observed.

5.4. Star formation history

5.4.1. Secular evolution of galaxies

Given the strong relationship between the secular evolution of the star formation history of galaxies and their total dynamical or stellar mass (Cowie et al. 1996; Gavazzi et al. 1996; Boselli et al. 2001; Gavazzi et al.
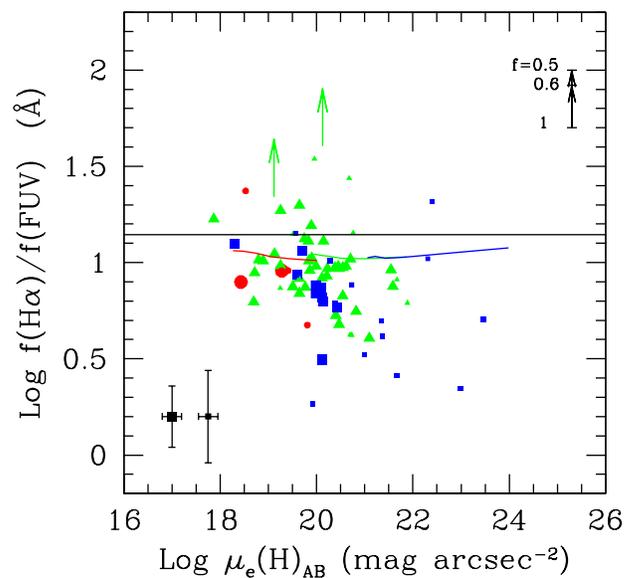

FIG. 7.— The relationship between the Hα to FUV flux ratio and the H band effective surface brightness for normal, late-type galaxies. Symbols and lines are coded as in Fig. 6.

2002b), we should first consider whether long term variations of the star formation activity of the target galaxies, which span four orders of magnitude in stellar mass, might induce variations in the Hα to FUV flux ratio. To do that we plot the variation of the Hα to FUV flux ratios as a function of the stellar mass (not shown), FUV-H colour, H band effective surface brightness[8] in Fig. 6 and 7 and compare the results to the predictions of the secular chemo-spectrophotometric models of galaxy evolution of Boissier & Prantzos (1999, 2000)[9]. As for the stellar mass, a trend is present when the Hα to FUV flux ratios is plotted vs. the FUV-H colour (99 % of probability that the two variables are correlated, Table 8) or

[8] Defined as the surface brightness within the effective radius, the radius including half of the total light (Gavazzi et al. 2000b)

[9] These models, computed assuming a Kroupa (2001) IMF, are done for galaxies with rotational velocities from 40 to 360 km s^{-1} and spin parameters $\lambda = 0.02$ (red solid line, for compact galaxies, $\lambda = 0.05$ (green solid line, for standard galaxies) and $\lambda = 0.09$ (blue solid line, for low surface brightness objects).
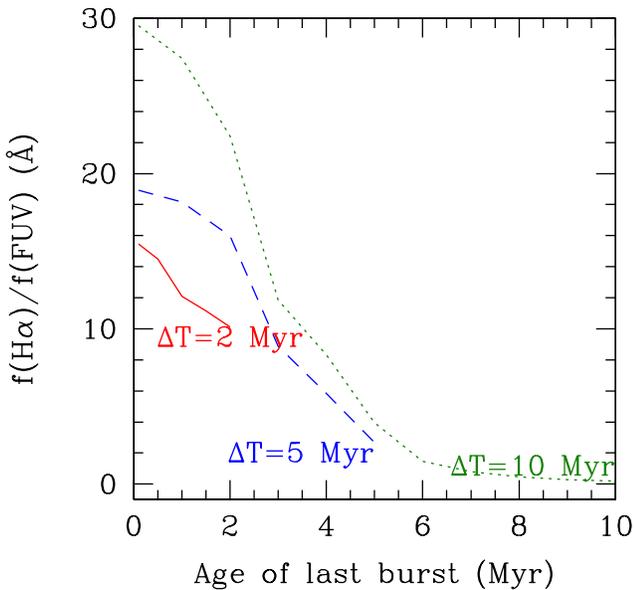
FIG. 8.— The variation of the Hα over FUV flux ratio as a function of the age of the last burst as expected for a galaxy whose emission is due to the contribution of subsequent instantaneous bursts of star formation (HII regions) every 2 (solid red), 5 (dashed blue) and 10 (dotted green) Myr.

the H band effective surface brightness (99%). Figures 6 and 7 indicate that the different secular evolution of the star formation activity of galaxies of different mass can induce variations in the Hα over FUV flux ratio only up to 0.1 dex and thus cannot explain the observed trends in the figures, where Log $f(H\alpha)/f(FUV)$ varies by 0.7 dex.

5.4.2. *Micro-history of star formation*

It has been claimed that the observed variation of the Hα over UV ratio in star forming regions in the outer disc of M81 is due to an age effect (Gogarten et al. 2009). An increase of the dispersion of the $f(H\alpha)/f(FUV)$ ratio in low mass galaxies is expected since in these objects the Hα emission is dominated by giant HII regions (Kennicutt 1988; Kennicutt et al. 1989) similar to 30 Doradus in the LMC which is responsible to ~

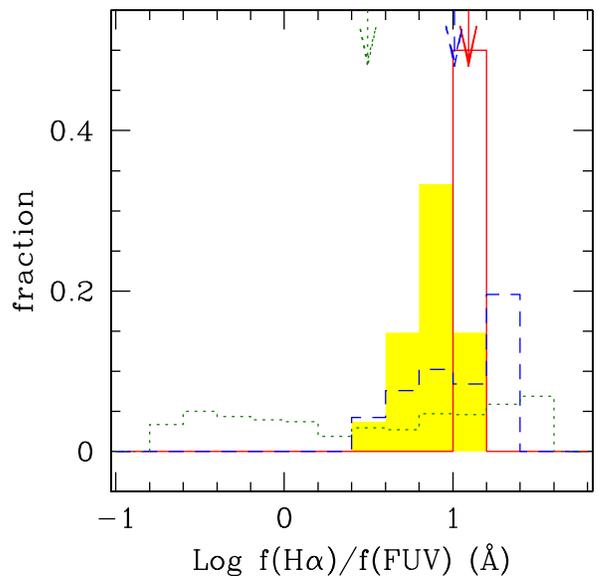
FIG. 9.— The expected distribution of the Hα over FUV flux ratio for a galaxy whose emission is due to the contribution of subsequent instantaneous bursts of star formation (HII regions) every 2 (solid red line), 5 (dashed blue line) and 10 (dotted green line) Myr compared to the observed distribution of normal, low mass ($M_{star} \leq 10^{9.2}$ M⊙) galaxies (yellow shaded histogram). Vertical arrows indicate the mean values.

50% of the galaxy emission[10] (Kennicutt et al. 1995). Given their short lifetime (some 10^6 years), comparable to that of the OB stars responsible for the Hα emission, with respect to that of the A stars emitting in FUV (~ 10^8 yrs), the probability of seeing a HII region still active in FUV but already quenched in Hα is relatively high. The observation of a galaxy whose dominant HII region is too old to be detected in Hα but not in FUV would easily lower its $f(H\alpha)/f(FUV)$ ratio by a factor of two in dwarfs, while the effect in massive spirals would be less than a few % just because the Hα emission is never dominated by a single HII region.

[10] The contribution of 30 Doradus to the total Hα emission of the LMC might even be larger if we consider that an important fraction of the diffuse emission of the galaxy, which is 35% of the total, might result from the ionization of the diffuse ISM due to the leakage of photons produced in giant HII regions.

Local age effects could thus contribute to the observed variation of the Hα to FUV flux ratio with stellar mass observed in Fig. 2. There are indeed some observational evidences that HII regions located along spiral arms are on average younger than those observed in low density regions such as the interarm, the outer discs of high surface brightness galaxies or those in low surface brightness objects (von Hippel & Bothun 1990; Oey & Clarke 1998; Helmboldt et al. 2008). This evidence is probably related to the fact that the youngest HII regions located along the spiral arms are those newly formed during the increase of the gas column density induced by the spiral wave. Being formed through induced star formation, they are now undergoing a burst of activity. Those in the interarm region were previously formed during the last crossing of the density wave[11]. Similarly, HII regions in the outer discs of spirals, in low surface brightness Im galaxies and in BCDs are sporadically formed thus on average older (~ 6 Myr) than those belonging to spiral arms that can be considered as coeval (≤ 1 Myr, Helmboldt et al. 2008; Tamburro et al. 2008). As for the observed decrease of the Hα E.W. of HII regions sporadically formed (von Hippel & Bothun 1990), we could expect that the same HII regions have a lower Hα to FUV flux ratio with respect to those still undergoing a starburst since formed through an induced process (HII regions in spiral arms). Indeed after 6 Myr the Hα flux is expected to drop by a factor of ~ 30 while the FUV flux remains almost constant.

To check whether a change in the micro history might be at the origin of the observed variation of the Hα over FUV flux ratio, we simulate the bursty star formation activity of a galaxy by considering the contribution of single HII regions treated as subsequent instantaneous bursts of intensity 10^4 M⊙ yr^{-1} repeated every ΔT years. These toy-models have been computed using the Starburst99 code (Leitherer et al. 1999; Vázquez & Leitherer 2005) with a Kroupa (2001) IMF and a solar metallicity (but we checked that metallicity has little influence). We then suppose that the total emission of a galaxy is the sum of the contribution of the different generations of HII regions[12] formed during the time, with the Hα emission dominated by the last generation of HII regions, while all HII regions formed during about the last 100 Myr contribute to the FUV emission. If, as in the case of massive galaxies, HII regions are formed at a constant rate with a frequency higher than the life time of the ionizing OB stars (10^7 yrs) (induced star formation), the resulting Hα over FUV ratio is $\sim$ constant and corresponds to the value determined for a constant star formation activity. In low luminosity systems, where HII regions are sporadically formed with a time delay longer than the age of the ionizing stars, the observed Hα over FUV ratio depends on the age of the last burst which only dominates the Hα emission of

the galaxy.

This is well illustrated in Fig. 8, which shows the expected variation of the Hα over FUV flux ratio as a function of the age of the last burst for a galaxy with an activity due to subsequent, instantaneous bursts of star formation happening every ΔT years.

Decreasing the frequency of the bursts from $\Delta T = 2$ (solid red), 5 (dashed blue) and 10 (dotted green) Myr increases the Hα over FUV flux ratio *at the epoch of the last burst* just because the contribution of the previous bursts to the UV emission is less and less important (they were less frequent in the past for $\Delta T = 10$ than for $\Delta T = 2$ Myr). However, the *probability* of observing galaxies with a lower Hα over FUV flux ratio (theoretical histograms in Fig. 9 are computed assuming every ages of the last burst within the range 0 to ΔT have the same probability to occur) increases just because of the longer interval of time in between two bursts. Figure 9 gives the probability distribution of observing a given $f(H\alpha)/f(FUV)$ flux ratio (in logarithmic scale) for galaxies with HII regions forming every $\Delta T = 2$ (solid red), 5 (dashed blue) and 10 (dotted green) Myr.

Figure 9 and Table 9 show that the different type of star formation, constant in massive late-type galaxies while sporadic in low mass systems, can induce on average a decrease of the Hα to FUV flux ratio of ~ 40 % (from *constant* to ΔT=10 Myr), a variation more important than that observed in our sample (0.14 dex). Furthermore for a sporadic star formation activity ($\Delta T \geq 5$ Myr) the distribution of the $f(H\alpha)/f(FUV)$ flux ratio is expected to be more spreaded than for a constant activity, including both high values of Hα to FUV flux ratios in the case of very young episods (ongoing starbursts) and low values whenever the age of the last burst is ≥ 2 Myr. While in low mass galaxies ($M_{star} \leq 10^{9.2}$ M⊙) the observed distribution of Log $f(H\alpha)/f(FUV)$ (yellow shaded histogram in Fig. 9) extends to values as low as 0.5 Å, values higher than the expected ratio for a constant activity (Log $f(H\alpha)/f(FUV) \geq 1.2$ Å) are not present since systematically excluded as starburst galaxies[13]. Values of ΔT in between 0 and 10 Myr are realistic since they give an average age of HII regions between 0 and 5 Myr, consistent with the observations (Helmboldt et al. 2008; Tamburro et al. 2008).

In late-type galaxies the surface brightness and the colour are proxies of morphology. The observed relation between $f(H\alpha)/f(FUV)$ and the effective surface brightness $\mu_e(H)$ shown in Fig. 7 (and colour in Fig. 6) might thus be due to the decreasing relative contribution of young to old HII regions to the total Hα luminosity of spiral galaxies of later types, i.e. characterized by a decreasing surface brightness (and bluer colour). Being the H band surface brightness and the FUV-H colour correlated with the galaxy stellar mass (Gavazzi et al. 1996), the same effect might be at the origin of the observed $f(H\alpha)/f(FUV)$ vs. M_{star} relation shown in Fig. 2.

Finally, we note that a similar explanation (burst phases separated by long quiescent periods) was advanced in Boissier et al. (2008) to explain the FUV-NUV

---

[11] The timescale between the passage of spiral density waves is of the order of ~ 40 Myr at any location along the disc (Rand 1993), a timescale longer than the expected life of HII regions (Oey & Clarke 1998).

[12] This assumption is reasonable since the diffuse emission of late-type galaxies, that can contribute up to 50% of the total Hα emission, is probably due to the leakage of ionizing photons from HII regions (Oey et al. 2007).

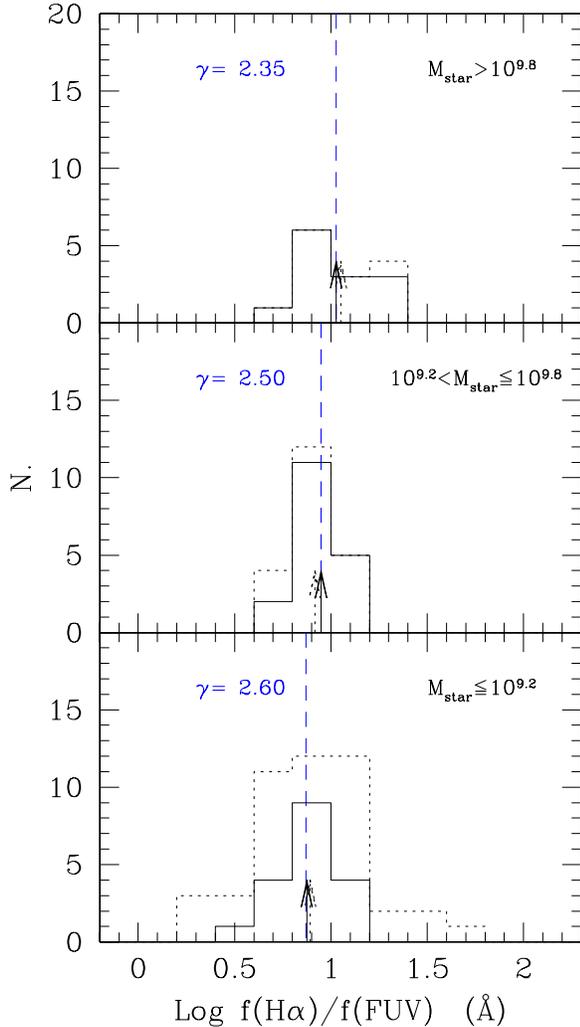[13] Log $f(H\alpha)/f(FUV) = 0.87 \pm 0.17$ Å for normal and 0.99 ± 0.26 Å for starburst, low mass galaxies.

FIG. 10.— The Hα to FUV flux ratio distribution (in logarithmic scale) for normal, late-type galaxies with high (solid line) and medium (dotted line) quality data in three different intervals in stellar mass: massive ($M_{star} > 10^{9.8}$ M⊙; upper panel), intermediate mass ($10^{9.2} < M_{star} \leq 10^{9.8}$ M⊙; central panel) and low mass ($M_{star} \leq 10^{9.2}$ M⊙; upper panel) galaxies. The vertical arrows indicate the mean values of the distributions (see Table 5). The vertical dashed line gives the γ slope for a Salpeter IMF.

colour of some Low Surface Brightness galaxies (only the delay between bursts was of the order of 100 Myr to affect FUV-NUV instead of 10 Myr for the Hα to FUV flux ratio).

5.5. Initial mass function

The determination of the SFR of galaxies using standard recipes as those given by Kennicutt (1998) resides on the hypothesis that galaxies have a constant initial mass function (IMF). Several new evidences, however, questioned this general statement.

The relative number of ionizing to non ionizing stars would decrease in dwarf systems if these objects have a steeper (or truncated) IMF compared to the Kennicutt one, as claimed by Hoversten & Glazebrook (2008) and Meurer et al. (2009). Figures 10 and 11 show that a vari-
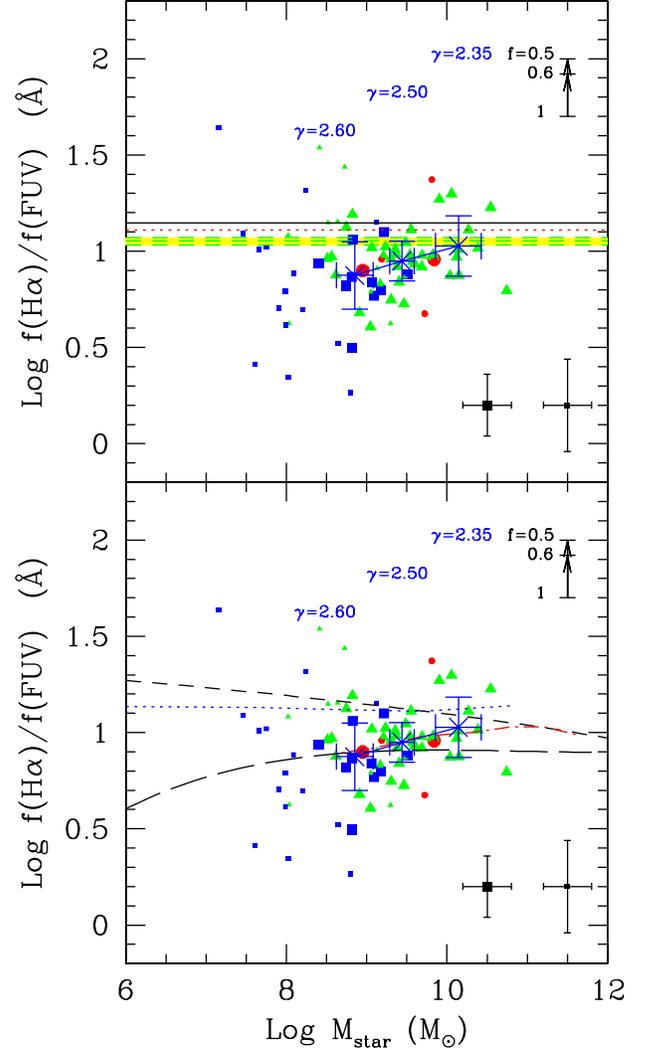

FIG. 11.— The relationship between the Hα to FUV flux ratio (in logarithmic scales) and the total stellar mass for "normal" late-type galaxies. Symbols are as in Fig. 5. Data are compared to the prediction of constant (upper panel) and variable (lower panel) IMF. The big, blue crosses indicate the mean values of Log $f(H\alpha)/f(FUV)$ as determined from our high quality sample in three different intervals of stellar mass, $M_{star} > 10^{9.8}$, $10^{9.2} < M_{star} \leq 10^{9.8}$, $M_{star} \leq 10^{9.2}$ M⊙. The γ values are the slope of the IMF assuming a mass range between 0.1 and 100 M⊙ (adapted from Meurer et al. (2009)). Upper panel: the black solid line gives the expected ratio for the Kennicutt (1998) calibrations, the red dotted line for a Kroupa (2001) IMF, the yellow shaded region is for a Salpeter (γ=2.35, M_{up}=100 M⊙) IMF as determined using three different stellar population models, where the green, dashed lines are, from top to bottom, GALAXEV (Bruzual & Charlot 2003), Starburst99 (Leitherer et al. 1999) and PEGASE (Fioc & Rocca-Volmerange 1997) (adapted from Meurer et al. 2009). Lower panel: the blue dotted line indicates a Bicker & Fritze-Alvensleben (2005) IMF, the black short-dashed line a Leitherer (2008) IMF, both determined assuming a metallicity-mass relation (see text). The black, long-dashed line shows the expected variation of Log $f(H\alpha)/f(FUV)$ vs. stellar mass for the integrated galaxy IMF of Pflamm-Altenburg et al. (2007; 2009), the blue dotted line for the proposed luminosity dependent IMF of Hoversten & Galzebrook (2009).

ation of the slope of the IMF from $\gamma = 2.35$ (Salpeter) in massive galaxies down to $\gamma = 2.60$ (or equivalently a decrease of the upper mass cutoff) in low mass systems (assuming $f = 1$) would be enough to reproduce the observed trend. These values are consistent with those proposed by Hoversten & Glazebrook (2008) (red dashed-dotted line in Fig. 11) but very different from those proposed Meurer et al. (2009), where γ has to change from ~ 1.5 to ~ 3.5 (if the upper mass cutoff is kept constant) to reproduce their observed variation in the Hα to FUV flux ratio. A non universal IMF could thus easily explain the observed trends.

In massive galaxies ($M_{star} > 10^{9.8}$ M$\odot$), where star formation can be considered as constant, Log $f(H\alpha)/f(FUV) = 1.03 \pm 0.16$ Å. This value can be compared to the expected ratios for different constant IMF: 1.07, 1.05 or 1.03 Å for a Salpeter IMF (with M_{up}=100 M$\odot$) using respectively the population synthesis models GALAXEV (Bruzual & Charlot 2003), Starburst99 (Leitherer et al. 1999) and PEGASE (Fioc & Rocca-Volmerange 1997), 1.15 Å is the value predicted by Kennicutt (1998) still using a Salpeter IMF and 1.11 Å for Kroupa (2001). All these predicted values are larger than the observed value in massive galaxies, and are thus consistent with the observations since f is ≤ 1.

5.5.1. *Integrated galactic initial mass function*

Pflamm-Altenburg and collaborators, based on statistical considerations, have recently questioned the universality of the IMF when considered as an integrated value for a given galaxy (IGIMF), a function appropriate for describing the IMF of unresolved galaxies such as those studied in extragalactic astronomy and cosmology. It has been shown that the maximum stellar mass in star clusters is limited by the mass of the cluster, and that the mass of the cluster itself is constrained by the star formation rate. Combining these considerations, Pflamm-Altenburg et al. (2007) have shown that the form of the integrated galactic initial mass function IGIMF is not universal but rather depends on the SFR of the parent galaxy. They thus concluded that using constant SFR(Hα) vs. $L(H\alpha)$ calibrations would lead to a systematic and significant (up to 3 orders of magnitude!) underestimate of the SFR, in particular in dwarf systems. The non-linear regime of the SFR(Hα) vs. $L(H\alpha)$ relation is expected for Hα luminosities $L(H\alpha) \leq 10^{40}$ erg s^{-1}, the typical range for galaxies with $M_{star} \leq 10^{8.5}$ M$\odot$. Although in a smaller way than for Hα, the variation of the IGIMF is also expected to affect the UV non-ionizing radiation (Pflamm-Altenburg et al. 2009), thus to modify the Hα to FUV flux ratio (black, long dashed line in Figure 12). The observed weak trends in the data are consistent with the expected variations of Log $f(H\alpha)/f(FUV)$ with the Hα and FUV luminosities or with the SFR, here determined using the average between the Hα and FUV estimates based on both the Pflamm-Altenburg et al. (2007; 2009; SFR_{PA}) and Kennicutt (1998) calibrations.

Using the tight SFR vs. M_{star} relation (SFR (M$\odot$ yr^{-1}) = $0.92\times$ LogM_{star} (M$\odot$) - 8.8, where the SFR is determined using the standard Kennicutt calibrations) observed in our sample, we can see whether the observed $f(H\alpha)$ over $f(FUV)$ flux ratio vs. M_{star} relation shown

in Fig. 11 is due to the variation of the IGIMF (long dashed line). A varying IGIMF should induce a decrease of $f(H\alpha)/f(FUV)$ for galaxies with stellar masses $M_{star} \sim \leq 10^{8.5}$ M$\odot$, while for galaxies with higher masses $f(H\alpha)/f(FUV)$ should have a constant value of ~ 8 Å. The large dispersion in the data plotted in Fig. 11 and 12 and the relatively small dynamic range in star formation of our target galaxies do not allow us to discriminate between a constant or a star forming dependent IMF. In massive galaxies the expected value of the Hα to FUV flux ratio for an IGIMF (standard model) is Log $f(H\alpha)/f(FUV) = 0.91$ Å, a value lower more than one σ from the observed distribution if $f < 0.91$. The IGIMF seems thus to be rejected (1 σ confidence level) if more than $\sim 10\%$ of the ionizing radiation is absorbed by dust.

5.5.2. *IMF vs. gas column density*

Theoretical considerations lead Krumholz & McKee (2008) to predict that only gas clouds with column densities ≥ 1 g cm^{-2} can avoid fragmentation and form massive stars. For this reason they expect a truncation of the IMF in low density regimes such as the outer discs of spiral galaxies which would almost suppress the Hα emission while only decrease the UV one. Extended UV discs without Hα emission have been indeed observed by GALEX in several nearby galaxies (Thilker et al. 2007, Boissier et al. 2007). Krumholz & McKee (2008) claim that for this reason a possible decrease of the $f(H\alpha)/f(FUV)$ ratio could be also expected in those objects not dominated by giant clouds such as dwarf galaxies.

To test this hypothesis we see whether the $f(H\alpha)/f(FUV)$ ratio is related to the total gas column density of our sample galaxies with the assumption that the total gas column density scales as the local gas density, which in star forming regions is significantly higher. Gas profiles are available only for a bunch of objects from the HI surveys of Warmels (1986) and Cayatte et al. (1994). By comparing their optical and HI distributions, however, we determined a general relation linking their optical to their HI diameter. Figure 13 shows the relationship between the $f(H\alpha)/f(FUV)$ ratio and the observed (upper panel) and inferred (lower panel) total gas surface densities of the target galaxies. The data do not show any relationship between the Hα to FUV ratio and the total gas column density. Because of gas dilution on the scale of galactic discs, however, the measured gas column densities are a factor of $\sim 10^3$ smaller than those needed for high mass star formation (≥ 1 g cm^{-2}). It is thus likely that the total gas column density here determined is not a good proxy of the local gas density. High resolution data are thus needed to check the validity of this theory.

5.5.3. *IMF vs. redshift*

Galaxy formation models based on cold gas accretion (Brinboim & Dekel 2003; Keres et al. 2005; Dekel et al. 2009) predict that the star formation rate is a fairly steady function of time (e.g. Finlator et al. 2006; Finlator et al. 2007), with a tight relationship between stellar mass and star formation activity, slightly evolving with redshift. Observations (e.g. Noeske et al. 2007; Elbaz et al. 2007; Daddi et al. 2007), however, revealed that
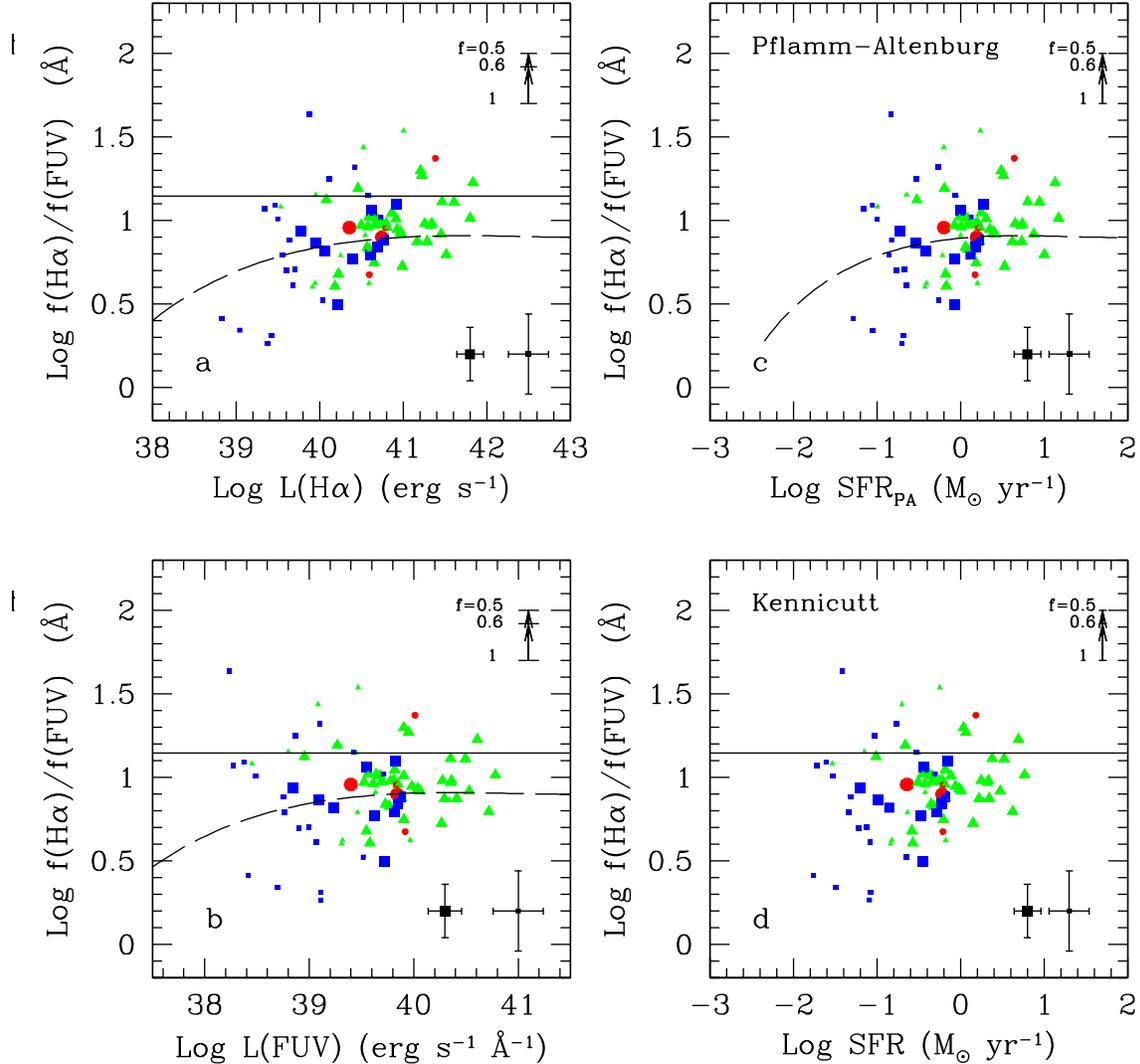
FIG. 12.— The relationship between the Hα to FUV flux ratio and the a) Hα luminosity, b) the FUV luminosity, c) the average Hα and FUV star formation rate as determined using the luminosity dependent calibration of Pflamm-Altenburg et al. (2007; 2009) and d) the average Hα and FUV star formation rate as determined using the Kennicutt (1998) calibration for the normal, late-type galaxies. Symbols are coded as in Fig. 5. The black, long dashed line represents the expected variations predicted by Pflamm-Altenburg et al. (2007; 2009) (standard model).

the amplitude of the M_{star} vs. SFR relation evolve with time in a way inconsistent with model predictions. Going to high redshift the observed SFRs are higher and/or the stellar masses are lower than predicted by models (Davé 2008; Wilkins et al. 2008). To justify this observational evidence several authors proposed that the IMF is not universal but rather evolving with time, being top heavy at high redshift (Larson 1998; Baugh et al. 2005; Davé 2008; Lacey et al. 2008; Wilkins et al. 2008) when the universe was dominated by starbursts (Rieke et al. 1993; Parra et al. 2007). Given the large uncertainties in the dust extinction correction for starbursts, the present analysis can not be used to infer any variation of the IMF with cosmic time.

6. CONCLUSION

We have studied the high mass star formation activity of an optically/near-IR selected sample of late-type

galaxies using two independent, direct tracers of star formation, the Hα and the FUV luminosity. This analysis brought the following results:

1) The distribution of the Hα over FUV flux ratio is highly dispersed (Log $f(H\alpha)/f(FUV) = 1.10 \pm 0.34$ Å) when the data are properly corrected for dust attenuation using the Balmer decrement and the TIR to FUV flux ratio. The dispersion increases (Log $f(H\alpha)/f(FUV) = 1.00 \pm 0.41$ Å) when are included data corrected using statistical recipes. This result indicates that Hα and UV luminosities, if blindly combined with standard recipes as those given by Kennicutt (1998), give star formation rates with at best an uncertainty of a factor of $\sim$ 2-3 depending on the applied dust attenuation correction. The error is significantly reduced (Log $f(H\alpha)/f(FUV) = 0.94 \pm 0.16$ Å) once AGN, star-
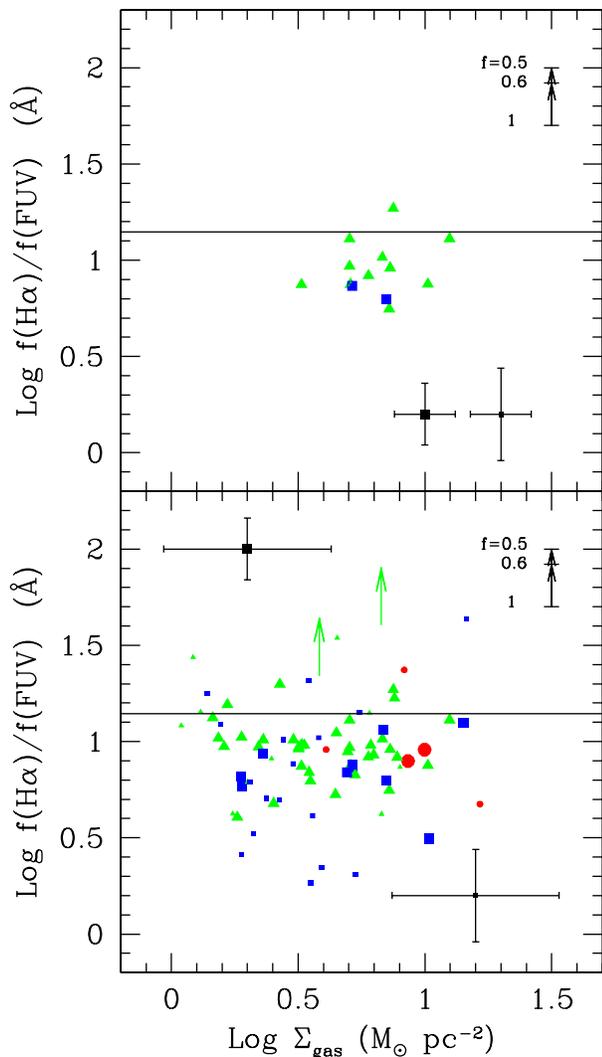
Fig. 13.— The relationship between the Hα to FUV flux ratio and total gas surface density for galaxies with available HI maps (upper panel) and for objects where the gas surface density has been inferred using a standard relation between the HI and the optical diameters (lower panel). Symbols are coded as in Fig. 5.

burst and highly inclined late-type galaxies are excluded.

2) Highly inclined galaxies, generally characterized by prominent dust lanes, have Hα over FUV flux ratio significantly higher (Log $f(H\alpha)/f(FUV) = 1.44 \pm 0.32$ Å) than normal, late-type galaxies. This result suggests that the dust attenuation corrections applied to this particular class of objects is wrong, probably because the assumption of isotropy in the UV emission of the galaxy is not correct (Panuzzo et al. 2003) or because the Balmer decrement does not give an accurate estimate of the extinction (photon leakage and/or porosity in the ISM).

3) Extinction is the major source of uncertainty in the determination of the Hα to FUV flux ratio even in normal, late-type galaxies. A direct measure of the Balmer decrement and, to a lesser extent, of the

TIR/FUV flux ratio are mandatory for avoiding any residual, systematic effect in the determination of the emitted Hα and FUV fluxes, thus on the star formation activity of the target galaxies.

4) The data are consistent with a Kennicutt (1998), Kroupa (2001) and Salpeter IMF. To match the data, the fraction of ionizing photons absorbed by dust (1-f) should be smaller than previously estimated (f=0.57, Hirashita et al. 2003), with f ranging from ~ 1 for a Salpeter IMF to 0.77 for Kennicutt (1998). The star formation dependent IGIMF proposed by Pflamm-Altenburg et al. (2007; 2009) can be hardly constrained because of the low dynamic range in star formation of our sample. We can only state that the proposed IGIMF is rejected (at 1 σ level) in massive galaxies if $f < 0.91$.

5) The Hα over FUV flux is barely related with stellar mass, FUV-H colour, H band effective surface brightness, star formation rate and gas fraction in normal, late-type galaxies. The steepness of these relationships increases if a mass/metallicity dependent f factor is assumed. With the present dataset it is impossible to state whether these trends are real or due to a residual in the adopted extinction corrections. If real, these trends can be explained by a small variation in the IMF, with a slope $\gamma \sim 2.35$ in massive systems and $\gamma \sim 2.60$ in dwarfs if f=1, while larger variations should be invoked if $f< 1$ in massive galaxies. We have however shown that the different micro history of star formation in giant, high surface brightness galaxies, characterized by induced star formation along their spiral arms, with respect to dwarf, low surface brightness systems where the ionizing and non ionizing UV emission is dominated by sporadically formed, giant HII regions can explain all the observed trends previously described.

The consequences of these results are major not only in the study of the star formation properties of nearby galaxies but also in a cosmological context as, for example, in the determination of the cosmic variation of the star formation activity of the universe. We indeed give an accurate estimate of the error on the star formation activity of galaxies using standard recipes based on two among the most widely used tracers, Balmer lines and UV luminosities. Variations in the IMF, as those claimed by Meurer et al. (2009) and Hoversten & Galzebrook (2008), which would have drastic consequences in the determination of the mass assembly through stellar formation during the evolution of the universe, are no more required to explain the observations. This micro history variation scenario, here proposed to explain the observed trends, should be tested in the study of the HII distribution of different nearby galaxies spanning a large range in morphological type, luminosity and surface brightness. If confirmed, its more direct consequence would be that the star formation activity of dwarf galaxies, although almost constant on long time scales (Sandage 1986; Gavazzi et al 1996; Boselli et al. 2001), is bursty on short times scales. The stationarity condition required for transforming Hα and UV luminosities into star formation rates would thus not be satisfied in these low luminosity systems, for which other techniques such as SED fitting would be required for measuring their activity.

REFERENCES

Baugh, C. M., Lacey, C. G., Frenk, C. S., Granato, G. L., Silva, L., Bressan, A., Benson, A. J., & Cole, S. 2005, MNRAS, 356, 1191
Bicker, J., Fritze-Alvensleben, U., 2005, A&A, 443, l19
Binggeli B., Sandage A., Tammann G., 1985, AJ, 90, 1681
Birnboim, Y., & Dekel, A. 2003, MNRAS, 345, 349
Bland-Hawthorn, J., Maloney, P., 1999, ApJ, 510, L33
Boissier, S., & Prantzos, N. 1999, MNRAS, 307, 857
Boissier, S. & Prantzos, N., 2000, MNRAS, 312, 398
Boissier, S., Boselli, A., Prantzos, N., & Gavazzi, G. 2001, MNRAS, 321, 733
Boissier, S., Prantzos, N., Boselli, A. & Gavazzi, G., 2003, MNRAS, 346, 1215
Boissier, S., Gil de Paz, A., Boselli, A., et al., 2007, ApJS, 173, 524
Boissier, S., et al. 2008, ApJ, 681, 244
Boselli, A., 2007, in "Astronomical Spectroscopy and Virtual Observatory", ed. M. Guainazzi
Boselli, A. & Gavazzi, G., 2002, A&A, 386, 124
Boselli, A. & Gavazzi, G., 2006, PASP, 118, 517
Boselli A., Casoli F., Lequeux J., 1995, A&AS, 110, 521
Boselli A., Tuffs R., Gavazzi G., Hippelein H., Pierini D., 1997, A&A 121, 507
Boselli, A., Gavazzi, G., Franzetti, P., Pierini, D., Scodeggio, M., 2000, A&AS, 142, 73
Boselli, A., Gavazzi, G., Donas, J., Scodeggio, M., 2001, AJ, 121, 753
Boselli, A., Iglesias-Páramo, J., Vilchez, J.M., Gavazzi, G., 2002a, A&A, 386, 134
Boselli A., Lequeux J., Gavazzi G., 2002b, A&A, 384, 33
Boselli A., Gavazzi G., Sanvito G., 2003, A&A, 402, 37
Boselli, A., Cortese, L., Deharveng, JM., et al., 2005, ApJ, 629, L29
Boselli A., Boissier, S., Cortese, L., Gil de Paz, A., Seibert, M., Madore, B., Buat, V., Martin, C., 2006, ApJ, 651, 811
Boselli A., Boissier, S., Cortese, L., Gavazzi G., 2008, A&A, 489, 1015
Boselli A., Eales, S., Chanial, P., et al., 2009, PASP, submitted
Bruzual, G., & Charlot, S. 2003, MNRAS, 344, 1000
Buat, V., Donas, J., Deharveng, JM., 1987, A&A, 185, 33
Buat, V., Xu, K., 1996, A&A, 303, 61
Buat, V., Boselli, A., Gavazzi, G., Bonfanti, C., 2002, A&A, 383, 801
Calzetti, D., 2001, PASP, 113, 1449
Cayatte, V., Kotanyi, C., Balkowski, C., van Gorkom, J., 1994, AJ, 107, 1003
Charlot, S., & Fall, S. M. 2000, ApJ, 539, 718
Charlot, S., Kauffmann, G., Longhetti, M., et al., 2002, MNRAS, 330, 876
Conroy, C., Gunn, J., & White, M., 2009a, ApJ, submitted (astroph/0809.4261)
Cortese, L., Boselli, A., Buat, V., et al., 2006, ApJ, 637, 242
Cortese, L., Boselli, A., Franzetti, P., et al., 2008, MNRAS, 386, 1157
Cowie, L., Songaila, A., Hu, E., Cohen, J., 1996, AJ, 112, 839
Daddi, E., et al. 2007, ApJ, 670, 156
Davé, R. 2008, MNRAS, 385, 147
Decarli, R., Gavazzi, G., Arosio, I., et al., 2007, MNRAS, 381, 136
Deharveng, JM., Buat, V., Le Brun, V., et al., 2001, A&A, 375, 805
Dekel, A., et al. 2009, Nature, 457, 451
Dopita, M., Kewley, L., Heisler, C., Sutherland, R., 2000, ApJ, 542, 224
Elbaz, D., et al. 2007, A&A, 468, 33
Finlator, K., Davé, R., Papovich, C., & Hernquist, L. 2006, ApJ, 639, 672
Finlator, K., Davé, R., & Oppenheimer, B. D. 2007, MNRAS, 376, 1861

Fioc, M., & Rocca-Volmerange, B. 1997, A&A, 326, 950
Fioc, M., & Rocca-Volmerange, B. 1999, A&A, 344, 393
Garnett, D. R. 2002, ApJ, 581, 1019
Gavazzi, G., Boselli, A., 1996, Astro. Lett. and Communications, 35, 1
Gavazzi, G., Pierini, D., Boselli, A., 1996, A&A, 312, 397
Gavazzi, G., Catinella, B., Carrasco, L., Boselli, A., Contursi, A., 1998, AJ, 115, 1745
Gavazzi, G., Boselli, A., Scodeggio, M., Pierini, D., Belsole, E., 1999, MNRAS, 304, 595
Gavazzi, G., Franzetti, P., Scodeggio, M., Boselli, A., Pierini, D., 2000b, A&A, 361, 863
Gavazzi, G., Franzetti, P., Scodeggio, M., Boselli, A., Pierini, D., Baffa, C., Lisi, F., Hunt, L., 2000a, A&AS, 142, 65
Gavazzi, G., Zibetti, S., Boselli, A., Franzetti, P., Scodeggio, M., Martocchi, S., 2001, A&A, 372, 29
Gavazzi, G., Boselli, A., Pedotti, P., Gallazzi, A., Carrasco, L., 2002a, A&A, 396, 449
Gavazzi, G., Bonfanti, C., Sanvito, G., Boselli, A., & Scodeggio, M., 2002b, ApJ, 576, 135
Gavazzi, G., Boselli, A., Donati, A., Franzetti, P. & Scodeggio, M., 2003, A&A, 400, 451
Gavazzi, G., Zaccardo, A., Sanvito, G., Boselli, A. & Bonfanti, C., 2004, A&A, 417, 499
Gavazzi, G., Donati, A., Cuccati, O., Sabatini, S., Boselli, A., Davies, J., Zibetti, S., 2005a, A&A, 430, 411
Gavazzi, G., Boselli, A., van Driel, W., O'Neil, K., 2005b, A&A, 429, 439
Gavazzi, G., Boselli, A., Cortese, L., Arosio, I, Gallazzi, A., Pedotti, P., 2006, A&A, 446, 839
Gil de Paz, A., Boissier, S., Madore, B., et al., 2007, ApJS, 173, 185
Gogarten, S. M., et al. 2009, ApJ, 691, 115
Gonzalez-Delgado, R., Leitherer, C., 1999, ApJS, 125, 479
Jansen, R. A., Fabricant, D., Franx, M., & Caldwell, N. 2000, ApJS, 126, 331
Jarrett, T., Chester, T., Cutri, R., Schneider, S. & Huchra, J., 2003, AJ, 125, 525
Hayes, M., Ostlin, G., Atek, G., et al., 2007, MNRAS, 382, 1465
Heckman, T., Semback, K., Meurer, G., et al., 2001, ApJ, 558, 56
Helmboldt, J. F., Walterbos, R. A. M., Bothun, G. D., O'Neil, K., & Oey, M. S. 2009, MNRAS, 393, 478
Hirashita, H., Inoue, A., Kamaya, H., Shibai, H., 2001, A&A, 366, 83
Hirashita, H., Buat, V., Inoue, A., 2003, A&A, 410, 83
Hoversten, E., Galzebrook, K., 2008, ApJ, 675, 163
Kenney J.,Young J., 1988, ApJS 66, 261
Kennicutt, R., 1988, ApJ, 334, 144
Kennicutt, R., 1992, ApJ, 388, 310
Kennicutt, R., 1998, ARA&A, 36, 189
Kennicutt, R. C., Jr., Edgar, B. K., & Hodge, P. W. 1989, ApJ, 337, 761
Kennicutt, R., Bresolin, F., Bomans, D., Bothun, G., Thompson, I., 1995, AJ, 109, 594
Kereš, D., Katz, N., Weinberg, D. H., & Davé, R. 2005, MNRAS, 363, 2
Kewley, L., & Ellison, S., 2008, ApJ, 681, 1183
Kobulnicky, H., Kennicutt, R., Pizagno, J., 1999, ApJ, 514, 544
Kroupa, P., 2001, MNRAS, 322, 231
Kroupa, P., Tout, C. A., & Gilmore, G. 1993, MNRAS, 262, 545
Krumholz, M., McKee, C., 2008, Nat., 451, 1082
Kurucz, R. L., 1992, in Barbuy B., Renzini A., eds, Proc. IAU Symp. 149, The Stellar Populations of Galaxies. Kluwer, Dordrecht, p. 225
Iglesias-Páramo, J., Boselli, A., Gavazzi, G., Zaccardo, A., 2004, A&A, 421, 887
Iglesias-Páramo, J., Buat, V., Takeuchi, T., et al., 2006, ApJS, 164, 38

Inoue, A., Hirashita, H., Kamaya, H., 2000, PASJ, 52, 539

Lacey, C. G., Baugh, C. M., Frenk, C. S., Silva, L., Granato, G. L., & Bressan, A. 2008, MNRAS, 385, 1155

Larson, R. B. 1998, MNRAS, 301, 569

Lee, H.C., Gibson, B., Flynn, C., Kawata, D., Beasley, M., 2004, MNRAS, 353, 113

Lee, J., Gil de Paz, A., Tremonti, C., et al., 2009, submitted to ApJ

Leitherer, C., 2008, in IAU Symp. 255, Low-Metallicity Star Formation, ed. L. Hunt, S. Madden, & R. Schneider (Cambridge: CUP)

Leitherer, C., Ferguson, H., Heckman, T., Lowenthal, J., 1995, ApJ, 454, L19

Leitherer, C., et al. 1999, ApJS, 123, 3

Lequeux J., Rayo, J. F., Serrano, A., Peimbert, M., Torres-Peimbert, S., 1979, A&A, 80, 155

Lequeux J., Maucherat-Joubert, M., Deharveng, JM., Kunth, D., 1981, A&A, 103, 305

Lequeux J., 1988, in "Lecture Notes in Physics: Evolution of Galaxies; Astronomical Observations", EADN Astrophysics School I, Les Houches, France, eds. I Appenzeller, H Habing, P. Léna, p147

Martin, C., Fanson, J., Schiminovich, D., et al., 2005, ApJ, 619, L1

Massey, P., Johnson, K. E., & Degioia-Eastwood, K. 1995, ApJ, 454, 151

Mateo, M. L. 1998, ARA&A, 36, 435

McGaugh, S., 1991, ApJ, 380, 140

Meurer, G., Heckman, T., Calzetti, D., 1999, ApJ, 521, 64

Meurer, G. R., et al. 2009, ApJ, 695, 765

Moustakas, J., & Kennicutt, R. C., Jr. 2006, ApJS, 164, 81

Muñoz-Mateos, J.C., Gil de Paz, A., Boissier, S., et al., 2009, ApJ, in press

Noeske, K. G., et al. 2007, ApJ, 660, L43

Oey, M., Clarke, C., 1998, AJ, 115, 1543

Oey, M. S., et al. 2007, ApJ, 661, 801

Osterbrock, D. 1989, Astrophysics of Gaseous Nebulae and Active Galactic Nuclei, University Science Books (Mill Valley)

Panuzzo, P., Bressan, A., Granato, G. L., Silva, L., & Danese, L. 2003, A&A, 409, 99

Parra, R., Conway, J. E., Diamond, P. J., Thrall, H., Lonsdale, C. J., Lonsdale, C. J., & Smith, H. E. 2007, ApJ, 659, 314

Pflamm-Altenburg, J., Weidner, C., Krupa, P., 2007, ApJ, 671, 1550

Pflamm-Altenburg, J., Weidner, C., & Kroupa, P. 2009, MNRAS, 395, 394

Rand, R., 1993, ApJ, 410, 68

Renzini, A. 2005, The Initial Mass Function 50 Years Later, 327, 221

Rieke, G. H., Loken, K., Rieke, M. J., & Tamblyn, P. 1993, ApJ, 412, 99

Rowan-Robinson, M., & Crawford, J. 1989, MNRAS, 238, 523

Salim, S., Rich, M., Charlot, S., et al., 2007, ApJS, 173, 267

Salpeter, E. E. 1955, ApJ, 121, 161

Sandage, A. 1986, A&A, 161, 89

Scalo, J., 1986, FCPh, 11, 1

Scalo, J. 1998, The Stellar Initial Mass Function (38th Herstmonceux Conference), 142, 201

Selman, F. J., & Melnick, J. 2008, ApJ, 689, 816

Springob, C., Haynes, M., Giovanelli, R., Kent, B., 2005, ApJS, 160, 149

Sullivan, M., Treyer, M. A., Ellis, R. S., Bridges, T. J., Milliard, B., & Donas, J. 2000, MNRAS, 312, 442

Tamburro, D., Rix, H.-W., Walter, F., Brinks, E., de Blok, W. J. G., Kennicutt, R. C., & MacLow, M.-M. 2008, AJ, 136, 2872

Thilker, D., Bianchi, L., Meurer, G., et al., 2007, ApJS, 173, 538

Tremonti, C., Heckman, T., Kauffmann, G., et al., 2004, ApJ, 613, 898

Tuffs, R. J., Popescu, C. C., Völk, H. J., Kylafis, N. D., & Dopita, M. A. 2004, A&A, 419, 821

Van Zee, L., Salzer, J., Haynes, M., O'Donoghue, A., Balonek, T., 1998, AJ, 116, 2805

Vázquez, G. A., & Leitherer, C. 2005, ApJ, 621, 695

Vázquez, G., Leitherer, C., Schaerer, D., Meynet, G., Maeder, A., 2007, ApJ, 663, 995

von Hippel, T., Bothun, G., 1990, AJ, 100, 403

Warmels, R.H., 1986, HI properties of spiral galaxies in the Virgo cluster (Groningen: Rijksuniversiteit)

Wilkins, S., Hopkins, A., Trentham, N., Tojeiro, R., 2008, MNRAS, 391, 363

Witt, A., Gordon, K., 2000, ApJ, 528, 799

Young, J., Xie, S., Tacconi, L., et al., 1995, ApJS 98, 219

Zaritsky, D., Kennicutt, R., Huchra, J., 1994, ApJ, 420, 87

Zurita, A., Rozas, M., Beckman, J., 2000, A&A, 363, 9

TABLE 1
THE DATA COMPLETENESS IN THE SAMPLE

Sample	Balmer dec+TIR/UV	Balmer dec	TIR/UV
HRS[a]	40	46	63
Virgo	36	65	96
Atlas	35	37	39
Total	111	148	198

Notes:
a: excluding HRS galaxies in the Virgo cluster

TABLE 2
THE THREE QUALITY SAMPLES

Sample	N. galaxies	error on Log f(Hα)/f(FUV)	Selection criterion	Extinction correction
High quality	111(49)	0.16	Balmer decrement + TIR/FUV	Hα/Hβ + TIR/UV
Medium quality	148(81)	≤ 0.24	Balmer decrement	Hα/Hβ + colour dependent statistical corrections
Low quality	198(120)	≤ 0.34	A(Hα) vs.M$_{star}$ + colour dependent statistical corrections

Notes: the medium and low quality samples include also the higher quality samples. Values in parenthesis are for "normal" galaxies.

TABLE 3
THE MEAN VALUES OF THE Hα TO FUV FLUX RATIO

Sample	H.Q.		M.Q.		L.Q.	
	N.	$<$Log $f(H\alpha)/f(FUV)>$ (Å)	N.	$<$Log $f(H\alpha)/f(FUV)>$ (Å)	N.	$<$Log $f(H\alpha)/f(FUV)>$ (Å)
All	111	1.10 ± 0.34	148	1.05 ± 0.37	198	1.00 ± 0.41
AGN	23	1.23 ± 0.34	24	1.28 ± 0.42	32	1.34 ± 0.40
Starburst	33	1.15 ± 0.44	33	1.15 ± 0.44	35	1.16 ± 0.44
incl$>80^{O}$ [a]	9	1.44 ± 0.32	13	1.23 ± 0.44	15	1.11 ± 0.52
Normal	49	0.94 ± 0.16	81	0.93 ± 0.25	120	0.87 ± 0.32

Notes: a) including all highly inclined galaxies listed in Table 4.

TABLE 4
GALAXIES WITH A LOG $f(H\alpha)/f(FUV) > 1.35$ Å[a]

Highly inclined galaxies					
Name	type	Log M_{star}	Log $f(H\alpha)/f(FUV)$	incl	Comments
		M$\odot$	Å	^{o}	
NGC3424	SB(s)b:?;HII	9.81	1.70	78	Interacting system
NGC3683	SB(s)c?;HII	10.14	1.70	69	With prominent dust lane
NGC4517	SA(s)cd: sp	10.32	1.50	81	With prominent dust lane
NGC4631	SB(s)d	9.92	1.68	82	With prominent dust lane
NGC5348	SBbc: sp	9.09	1.55	90	With prominent dust lane
IC1048	S	9.72	1.72	74	
Starburst galaxies					
Name	type	Log M_{star}	Log $f(H\alpha)/f(FUV)$	F60/F100	Comments
		M$\odot$	Å		
NGC2798	SB(s)a pec;HII	9.87	3.08	0.70	Interacting system
M82	I0;Sbrst;HII	9.93	1.61	0.94	Interacting system
NGC4383	Sa? pec;HII	9.52	1.48	0.66	With peculiar Hα tails
UGCA284	BCD:	8.41	1.41	0.53	Single HII region
NGC5145	S?;HII;Sbrst	9.47	1.59	0.51	
NGC7771	SB(s)a;HII;LIRGSbrst	11.02	1.42	0.55	Interacting system

Notes: a = Log $f(H\alpha)/f(FUV) = 1.35$ Å is 2 σ higher than the mean value of normal, massive galaxies.

TABLE 5
The Hα to FUV flux ratio for normal, late-type galaxies of different mass

Sample	quality	N. obj.	$< \mathrm{Log}\, f(H\alpha)/f(FUV) >$ Å
$M_{star} > 10^{9.8}$ M⊙	high	13	1.03 ± 0.16
	medium	14	1.05 ± 0.18
$10^{9.2} < M_{star} \leq 10^{9.8}$ M⊙	high	18	0.95 ± 0.10
	medium	21	0.93 ± 0.13
$M_{star} \leq 10^{9.2}$ M⊙	high	18	0.87 ± 0.17
	medium	46	0.89 ± 0.30

TABLE 6
The Hα to FUV flux ratio vs. Log M_{star} relation using data corrected according to different recipes

Extinction	correction			
Hα	FUV	a	b	R[c]
Observed	Observed	0.13±0.05	-0.03±0.42	0.40
Hα/Hβ(TW)	FIR/UV(TW)	0.08±0.04	0.18±0.37	0.29
Hα/Hβ(TW)	Calzetti	-0.03±0.03	1.17±0.30	-0.08
Statistical[d]	FIR/UV(TW)	0.35±0.03	-2.27±0.30	0.85
Hα/Hβ(TW)	Statistical[d]	0.11±0.05	-0.15±0.43	0.32
Statistical[d]	Statistical[d]	0.38±0.04	-2.60±0.30	0.80

Notes: linear fit to the data: Log $f(H\alpha)/f(FUV)$ = a(X-variable) + b for the subset of 49 normal galaxies of the high quality sample.
c: linear correlation coefficient.
d: statistical corrections as those applied by Meurer et al. (2009).

TABLE 7
The f values for different IMF

IMF	Log $f(H\alpha)/f(FUV)$ Å	f
Kroupa 2001	1.11	0.84
Salpeter (0.1< m <100 M⊙) (Kennicutt 1998)	1.15	0.77
Salpeter (0.1< m <100 M⊙) (Starburst99)	1.05	0.95
Salpeter (0.1< m <100 M⊙) (PEGASE)	1.03	0.99
Salpeter (0.1< m <100 M⊙) (GALAXEV)	1.07	0.91

TABLE 8
The best fit to the data

High quality sample					
Log $f(H\alpha)/f(FUV)$ Å					
X-variable	a	b	R[c]	ρ [d]	%[e]
Log M_{star}	0.08±0.04	0.18±0.37	0.29	0.27	93.7
FUV-H	0.09±0.03	0.73±0.07	0.40	0.39	99.3
$\mu_e(H)$	-0.08±0.03	2.50±0.54	0.39	-0.37	98.9
12+Log(O/H)	0.05±0.14	0.51±1.22	0.05	0.02	10.5
Log $M_{gas}/(M_{gas} + M_{star})$	-0.36±0.09	0.81±0.04	0.50	-0.40	99.5
Log SFR	0.08±0.05	0.96±0.02	0.21	0.21	85.7
Medium quality sample					
Log $f(H\alpha)/f(FUV)$ Å					
X-variable	a	b	R[c]	ρ [d]	%[e]
Log M_{star}	0.06±0.04	0.37±0.37	0.19	0.21	90.8
FUV-H	0.09±0.04	0.73±0.09	0.29	0.35	99.6
$\mu_e(H)$	-0.09±0.03	2.73±0.60	0.35	-0.39	99.8
12+Log(O/H)	0.13±0.11	-0.21±0.98	0.14	0.10	59.0
Log $M_{gas}/(M_{gas} + M_{star})$	-0.39±0.12	0.81±0.04	0.38	-0.39	99.8
Log SFR	0.10±0.05	0.97±0.03	0.24	0.21	90.8

Notes: linear fit to the data: Log $f(H\alpha)/f(FUV)$ = a(X-variable) + b
c: linear correlation coefficient.
d: generalized Spearman's rank order correlation coefficient.
e: Spearman's probability that the two variables are correlated.

TABLE 9
THE EXPECTED $f(H\alpha)/f(FUV)$ DISTRIBUTION FOR SUBSEQUENT STARBURSTS

ΔT	<age>	$< f(H\alpha)/f(FUV) >$	$< \mathrm{Log}\ f(H\alpha)/f(FUV) >$
Myr	Myr	Å	Å
constant	-	12.8	1.11
2	1.05±0.55	12.5±1.7	1.09±0.06
5	2.55±1.41	11.8±5.6	1.01±0.25
10	5.05±2.86	9.0±10.1	0.49±0.74

Notes: for a Kroupa (2001) IMF with solar metallicity.

APPENDIX

A: THE OBSERVATIONAL DATA

The dataset used in the present analysis is composed of imaging and spectroscopic data covering the whole UV to IR spectral range. Hα+[NII] narrow band imaging of the HRS late-type galaxies has been recently obtained at the 2.1m San Pedro Martir telescope. Data for galaxies within the Virgo cluster region are available from our previous observations (Boselli & Gavazzi 2002; Boselli et al. 2002a; Gavazzi et al. 1998, 2002, 2006a), while those for the GALEX UV atlas of galaxies from different sources.

UV data have been taken thanks to GALEX in the two UV bands FUV ($\lambda_{\rm eff} = 1539$Å, $\Delta\lambda = 442$Å) and NUV ($\lambda_{\rm eff} = 2316$Å, $\Delta\lambda = 1069$Å). Observations have been taken as part of the Nearby Galaxy Survey (NGS; Gil de Paz et al. 2007), the Virgo cluster (Boselli et al. 2005), the All Imaging Survey (AIS) or as pointed observations in open time proposals.

Photometric data for the HRS and the GALEX atlas of galaxies have been taken from different sources in the literature. For all galaxies near-IR data are available from 2MASS (Jarrett et al. 2003). For the Virgo cluster region H (1.65 μm) and K (2.1 μm) band frames have been obtained during a near-IR imaging survey (Boselli et al. 1997; 2000; Gavazzi et al. 2000a, 2001). B and V frames are available for most of the analyzed galaxies thanks to our own observations (Gavazzi & Boselli 1996; Gavazzi et al. 2001; 2005a and Boselli et al. 2003). Fluxes at all wavelengths, including UV and Hα, were obtained using our own procedures by integrating all images within elliptical annuli of increasing diameter up to the optical B band 25 mag arcsec^{-2} isophotal radii.

A low resolution ($R \sim 1000$), integrated spectroscopic survey in the wavelength range 3500-7200 Å of the HRS is under way at the 1.93m OHP telescope. In order to sample the spectral properties of the whole galaxy, and not just those of the nuclear regions, observations have been executed using the drifting technique described in Kennicutt (1992). Exposures are taken while constantly and uniformly drifting the spectrograph slit over the full extent of the galaxy. A resolution $R \sim 1000$ is mandatory for resolving [NII] from Hα and estimating the underling Balmer absorption under Hβ. These data are combined with those available for the Virgo cluster region (Gavazzi et al. 2004) or for the UV GALEX atlas (Kennicutt 1992; Jensen et al. 2001; Mosutakas & Kennicutt 2006).

HI observations, needed for excluding the perturbed cluster galaxy population and for studying the relationship between the high mass star formation activity and the total gas content, are available for almost all the late-type galaxies in the HRS (Springob et al. 2005), in the Virgo cluster region (Gavazzi et al. 2005b) and in the UV GALEX atlas (Leda database). A ^{12}CO(1-0) survey of the HRS galaxies, necessary for determining their molecular gas content, is under way at the 12m Kitt Peak telescope. These data are combined with those available in the literature from the FCRAO survey of Young et al. (1995), Kenney & Young (1988) and Boselli et al. (1995; 2002b) for the Virgo cluster region. Far-infrared IRAS data at 60 and 100 μm, necessary for correcting UV and optical data for internal extinction, have been taken from different sources in the literature.

Most of data used in the present analysis relative to the Virgo cluster are available on the net on the GOLDMine database (Gavazzi et al. 2003).

B: THE DERIVED PARAMETERS

This dataset is used to derive different useful parameters of the selected galaxies: the ionizing and non-ionizing UV radiation, the stellar mass, the metallicity and the star formation rate (SFR). These entities can be determined only after applying some corrections to the observed data.

1) Extinction corrections: both Hα and UV data must be corrected for dust extinction. The attenuation in the Hα line ($A(H\alpha)$) can be measured using the Balmer decrement determined from the spectroscopic data. The high resolution ($R \sim 1000$) and high sensitivity of the data allow us to make an accurate determination of the underlying Balmer absorption under Hβ, a critical entity necessary for a correct estimate of the Balmer decrement (Kobulnicky et al. 1999; Gavazzi et al. 2004). The blending of the [NII] doublet prevents us from measuring the underlying absorption under Hα. We thus use a standard correction of 1.5 Å (Gavazzi et al. 2004). Upper limits are determined for those galaxies with Hα line emission and undetected Hβ. The integrated nature of the spectroscopic data is optimized for getting values representative of the whole galaxy, avoiding any systematic effect do to aperture corrections necessary when spectroscopic nuclear data are used. The attenuation of the Hα line is then measured using the galactic extinction law of Lequeux et al. (1979), as in Cortese et al. (2006). For galaxies without spectroscopic data we use a luminosity dependent extinction relation as determined for those galaxies with available data, plotted in Fig. 14 once the H band luminosity is transformed into stellar masses computed as below:

$A(H\alpha)$ (mag) $=1.22\times$Log L_H (solar units) - 11.28

Given the huge dispersion in this relation, we consider as highly inaccurate those Hα fluxes corrected without a direct measure of the Balmer decrement (low quality sample). The Hα flux should also be corrected to take into account that a fraction $(1-f)$ of the Lyman continuum photons is absorbed by dust before ionizing the atomic hydrogen. For consistency with other works we do not apply any f correction.

The UV attenuation ($A(UV)$) is determined using the recipes of Cortese et al. (2008) which are based on the idea that the UV radiation absorbed by dust is re-emitted in the far-IR. For those galaxies without far-IR data, $A(UV)$ is measured using the colour or surface brightness dependent relations given in Cortese et al. (2008). While the use of an energetic balance between the UV absorbed light and the far-IR emitted radiation is at present the most accurate
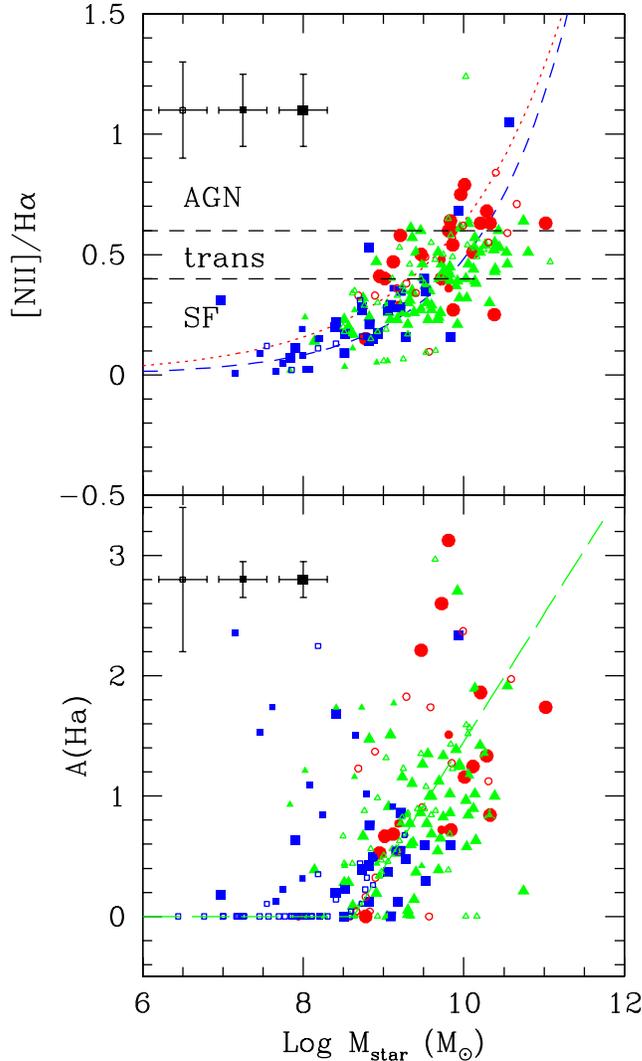
Fig. 14.— The relationship between a) the [NII]/Hα ratio and b) $A(H\alpha)$ and the stellar mass (in logarithmic scale). The horizontal, black dashed lines indicate the intervals in [NII]/Hα for AGN, transition and star forming galaxies. The red dotted line gives the empirical [NII]/Hα to stellar mass calibration given in Boselli et al. (2002b), the blue short-dashed line that of Decarli et al. (2007), while the green long-dashed line the $A(H\alpha)$ vs. Log M_{star} relation. The Decarli and the $A(H\alpha)$-L_H relations are used in this work whenever spectroscopic data are not available (low quality sample). Symbols are coded as in Fig. 5.

method for determining the UV dust attenuation in galaxies, the use of a colour or surface brightness dependent relation is quite indirect and still highly uncertain.

2) [NII] contamination in Hα+[NII] imaging data: narrow band Hα+[NII] imaging data, used for determining the total Hα flux of the selected galaxies, are corrected for [NII] contamination using the Hα/[NII] ratio measured from spectroscopic data. For those galaxies without any spectroscopic information, the Hα/[NII] ratio is determined assuming the luminosity dependent relation given in Decarli et al. (2007) and consistent with Boselli et al. (2002b). Hα fluxes statistically corrected for [NII] contamination are more uncertain than those based on spectroscopic data. The use of narrow band images and integrated spectra minimize aperture effects.

3) Stellar mass: Stellar masses are calculated using near-IR-optical colour dependent luminosity-mass relations as determined from our chemo-spectro-photometric models of galaxy evolution (Boissier & Prantzos 2000). The availability of near-IR magnitudes for almost all galaxies in the sample, a direct tracer of both the bulk of the stellar population and of the total dynamical mass of galaxies (Gavazzi et al. 1996), secure an accurate determination of the total stellar mass of the selected galaxies. The adopted relation, computed assuming a Kroupa (2001) IMF, is (with Johnson magnitudes in Vega system):

Log M_{star} (M⊙) - Log L_H (L$_H$⊙) = -1.08 +0.21(B-H)

We note that the grid of models was recomputed using the Kroupa (2001) IMF (rather than the Kroupa et al. (1993)

IMF as in Boissier & Prantzos 1999). This changes seems to improve the agreement with recent UV data in SINGS galaxies without producing huge modifications to other results (Muñoz-Mateos et al., in preparation).

4) Metallicity: Extinction corrected optical emission lines available from integrated spectra have been used to determine the metallicity of the observed galaxies using four different calibrations: van Zee et al. (1998), Dopita et al. (2000), Kobulnicky et al. (1999) and McGaugh (1991). The value used here is the mean value determined using these different calibrations.

5) Star Formation Rates (SFR): Hα and UV luminosities can be converted into star formation rates (in M$\odot$ yr^{-1}) using population synthesis models combined with some hypothesis concerning the star formation history, the IMF and the metallicity of the observed galaxies. For a given star formation history, metallicity and IMF, the relationship between the high mass star formation rate and the Hα and UV luminosities depends on the adopted population synthesis model. Here SFR are measured using the standard recipes of Kennicutt (1998) unless quoted differently, and are average values as determined using Hα and FUV data.

C: ERROR BUDGET

Observational errors as well as the different methods to derive the various parameters used in the following analysis are sources of uncertainties. Those mostly affecting our analysis are the uncertainties on the measure of the extinction corrected Hα and UV fluxes, thus on the Hα to FUV flux ratio, the variable analyzed in this work.

Hα flux: the typical error in the observed Hα+[NII] flux is ~ 0.15 mag; this includes both the uncertainty on the spectro-photometric zero point and on the sky background subtraction for the extraction of the total galaxy flux in extended sources. The correction for the [NII] contamination has a mean uncertainty of ~ 0.15 mag whenever integrated spectra are available, but up to ~ 0.20 mag when a statistical correction is applied. Extinction corrections using the observed Balmer decrement introduce an extra 0.15 mag uncertainty that increases to ~ 0.60 mag in the case of a statistical corrections. While the S/N increases with luminosity in both spectroscopic and narrow band imaging data, the underlying Balmer absorption, dust extinction and [NII] contamination are more severe in bright, massive galaxies. We thus expect that at a first order the uncertainty on the measured Hα flux of the target galaxies is ~ 0.26 mag (0.10 dex) whenever spectroscopic data are available, and ~ 0.65 mag (0.26 dex) elsewhere. Other sources of uncertainties hardly quantifiable are however present in the determination of the ionizing flux emitted by stars: these are the escape fraction and the fraction of ionizing photons absorbed by dust before they ionize the gas $(1 - f)$.

UV flux: the typical photometric error (zero point and flux extraction in extended sources) in the determination of the observed FUV and NUV fluxes is of the order of $\sim 15\%$, with slightly better values for galaxies observed in the MIS/NGS with respect to those observed during the AIS. The major source of uncertainty in the determination of the emitted UV fluxes is the extinction correction. The error on the correction is of the order of ~ 0.2 mag when IR data are available (this including $\sim 15\%$ error on the IRAS fluxes), and 0.5 mag when statistical corrections are applied (Cortese et al 2008). Considering an extra 0.20 mag uncertainty due to the adopted dust model (geometry, extinction curve...) the resulting error on the UV fluxes ranges from ~ 0.32 mag (0.13 dex) in galaxies with available far-IR data up to ~ 0.56 mag (0.22 dex) whenever more indirect recipes are applied.

Stellar masses: the photometric error on the near-IR magnitudes used on the determination of stellar masses is of the order of 0.10-0.15 mag, slightly larger on colours. The comparison of the mass determination using different spectro-photometric models of galaxy evolution have shown that differences in the determined stellar masses of evolved, late-type galaxies such as those analyzed in this work might be up to ~ 0.30 dex (Conroy et al. 2009a).

Metallicity: the estimated value of the metallicity of the observed galaxies is rather uncertain not only because of observational errors (flux extraction, extinction correction) but also because of the use of indirect calibrations. It is rather difficult to quantify this error (Kewley & Ellison 2008), that should be of the order of 0.20 in units of 12+Log(O/H) excluding the rather large uncertainties on the yields.

Other quantities: the error on the $(FUV - H)_{AB}$ colour and on the effective surface brightness $\mu_e(H)_{AB}$ is ~ 0.20 mag, while that on the gas column density is small, 0.12 dex, whenever HI maps are available, while large, up to 0.33 dex, when gas column densities are determined using data of unresolved objects. The error on the gas fraction is of the order of ~ 0.16 dex. The resulting error on the star formation activity of the target galaxies is of a factor of 2-3 when low quality data are used, 50 % using high quality data.

D: POSSIBLE SELECTION BIASES

The selected sample combined with the available incomplete set of data might introduce unwanted biases in out analysis. The [NII] emission contaminates the Hα emission mostly near the galaxy nucleus (Boselli 2007). The correction applied to the data does not take into account this effect. The use of integrated spectroscopic values combined with narrow band Hα+[NII] data should however minimize any major aperture effect. Furthermore we exclude in the following analysis AGNs, i.e. those galaxies where the [NII] contamination is more important.

A possible bias in the determination of the metallicity can result from the fact that, although we use the mean value of four different calibrations, the lack of the [OII] 3727 Å line (and sometimes of the [OIII] 5007 Å) in the massive galaxies forces us to use different calibrations as a function of the galaxy luminosity.

Because of the impossibility of a direct measure of the Hα underlying absorption on the spectra caused by the blending of the [NII] doublet, Hα fluxes in the spectroscopic data have been corrected using the canonical value of 1.5 Å. Detailed Balmer-line models by Kurucz (1992) indicate that the underlying absorption of the Hα and Hβ lines are similar within

30%. The underlying absorption under Hβ measured from our own data is slightly larger ($\sim$ 5 Å, Gavazzi et al. 2004), thus the applied correction might be underestimated. A possible bias, if present, is however expected to be small since given the line ratio of the Hα and Hβ lines (2.86 without extinction), the error on the Hα line is small in those objects where Hβ can be detected. Furthermore it has been shown that the Balmer underlying absorption does not depend sensitively on metallicity (Kurucz 1992; Gonzlez-Delgado & Leitherer 1999), thus this bias, if present, would hardly introduce any systematic trend with mass and metallicity.